The Synthesis of Higher Oxides of Alkalai and Alkaline Earth Metals in an Electric Discharge: Theoretical and Experimental Studies

by

Alexis T. Bell and
Pasupati Sadhukhan

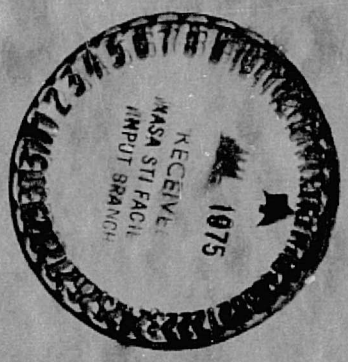

The Synthesis of Higher Oxides of Alkalai and Alkaline Earth Metals in an Electric Discharge: Theoretical and Experimental Studies

FINAL REPORT

for the period

June 1, 1971 through August 31, 1974

Submitted by

Alexis T. Bell
(Principal investigator)

and

Pasupati Sadhukhan

Department of Chemical Engineering
University of California, Berkeley, California 94720

This work was supported by the

National Aeronautics and Space Administration

under Grant NGR-05-003-462

and

NASA-Ames University Consortium
Interchange Agreement

NCAR-050-409

NASA Technical Officer:

Dr. Theodore Wydeven
Biotechnology Division
NASA-Ames Research Center
MS 239/4
Moffett Field, California 94035

UNIVERSITY OF CALIFORNIA, BERKELEY

BERKELEY • DAVIS • IRVINE • LOS ANGELES • RIVERSIDE • SAN DIEGO • SAN FRANCISCO

SANTA BARBARA • SANTA CRUZ

DEPARTMENT OF CHEMICAL ENGINEERING
BERKELEY, CALIFORNIA 94720

July 7, 1975

NASA Scientific and Technical
Information Facility
P.O. Box 8757
Baltimore/Washington International Airport
Baltimore, Maryland 21240

Gentlemen:

The attached Ph.D. thesis of Pasupati Sadhukhan represents the final report on the research undertaken to study the synthesis of higher oxides of alkalai and alkaline earth metals in an electric discharge. During the period of June 1, 1971 through August 31, 1974 this work was supported under NASA grant NGR-05-003-462 entitled "A Study of the Mechanism for the Formation of Higher Oxides of Alkalai and Alkaline Earth Metals in an Electric Discharge". The final phase of the work which covered the period June 1, 1974 through March 31, 1975 was supported under a NASA-Ames University Consortium Interchange Agreement NCAR-050-409 entitled "Development of Solid Oxygen Sources".

Three papers based upon Dr. Sadhukhan's research are now in preparation and will be submitted for publication. Copies of these manuscripts will be forwarded to the contract monitor and the NASA Scientific and Technical Information Facility as soon as they are ready.

Sincerely,

Alexis T. Bell

Alexis T. Bell
Associate Professor

ATB:new
encl.

The Synthesis of Higher Oxides of Alkali and Alkaline Earth Metals in an Electric Discharge: Theoretical and Experimental Studies

By

Pasupati Sadhukhan

B.Tech. (University of Calcutta) 1967
M.Tech. (University of Calcutta) 1968
M.S. (University of California) 1971

DISSERTATION

Submitted in partial satisfaction of the requirements for the degree of

DOCTOR OF PHILOSOPHY

in

Chemical Engineering

in the

GRADUATE DIVISION

of the

UNIVERSITY OF CALIFORNIA, BERKELEY

Approved:

Alexis T. Bell

W. Bartlet

D. N. Hanson

Committee in Charge

.....

ACKNOWLEDGEMENTS

It is a genuine pleasure to acknowledge my gratitude to Alexis T. Bell who, with his interest, friendly guidance and criticism, has aided in this investigation. Thanks are also due to Prof. Neil Bartlett and Theodore Wydeven for stimulating discussions on the chemistry of superoxides. The interest of Prof. Donald N. Hanson is also appreciated.

The author wishes to express his appreciation to all his colleagues in the laboratory, who have aided in this work.

Finally, the author is indebted to his wife, Maya who has patiently typed the thesis and helped him in many other ways.

TABLE OF CONTENTS

TABLE OF CONTENTS(continued)

TABLE OF CONTENTS(continued)

TABLE OF CONTENTS (continued)

LIST OF FIGURES

LIST OF FIGURES (continued)

LIST OF TABLES

THE SYNTHESIS OF HIGHER OXIDES OF ALKALI AND ALKALINE EARTH METALS IN AN ELECTRIC DISCHARGE: THEORETICAL AND EXPERIMENTAL STUDIES

Pasupati Sadhukhan

Dapartment of Chemical Engineering
University of California
Berkeley, California

ABSTRACT

Potassium hydroxide when subjected to the products of an electrical discharge sustained in oxygen produces both potassium peroxide and superoxide. The conversion to higher oxides strongly depends upon the particle size of KOH, the position of KOH in the discharge zone and the operating conditions of the discharge. The maximum conversion of KOH in terms of equivalent weight percent KO_2 is 75%.

Similar experiments performed with hydroxides of lithium and calcium do not form superoxides but instead are converted to peroxides. The yields of peroxides strongly depend upon the operating conditions of the discharge. The maximum yields of CaO_2 and LiO_2 are 82% and 94% by weight respectively.

The absence of superoxides and the presence of peroxides of lithium and calcium have been explained

from the consideration of relative thermodynamic stability of the oxides of lithium and calcium. The thermodynamics of $Ca(O_2)_2$ have been investigated theoretically while those of LiO_2 were taken from the literature. Both $Ca(O_2)_2$ and LiO_2 are found to be highly unstable with respect to lower oxides of each metal.

Although the reaction mechanism for the conversion of hydroxides to higher oxides can not be explained definitively, some of effects of discharge operating conditions on product yield can be interpreted if it is assumed that atomic oxygen is the primary oxidizing agent.

Finally, it was observed that Seyb and Kleinberg's method for determining the amounts of superoxide and peroxide present in a KO_2-K_2O_2 mixture does not give accurate results. For such mixtures thermogravimetric analysis (TGA) has been shown to provide a more accurate means for determining the amount of KO_2.

The TGA analysis also served to reveal a number of interesting features related to the decomposition of KO_2-K_2O_2 mixtures. This decomposition is believed to occur by partial decomposition of the KO_2 at temperatures between 125 and 250°C, formation of a solid solution between the components between 250 and

350°C, decomposition of the residual KO_2 between 350°C and 500°C, and decomposition of K_2O_2 above 600°C. Interpretation of the features observed on the thermograms was assisted by differential thermal analyses.

CHAPTER 1

INTRODUCTION

Alkali and alkaline earth metals form a variety of oxides which are shown in Table 1. The oxides in each column are listed in the order of increasing proportion of oxygen to metal as one reads down the table. The oxides other than the monoxide are collectively called higher oxides. As indicated in Table 1 not all of the higher oxides have been synthesized to date. Furthermore the existence of lithium and magnesium superoxides are not clearly established (1) and ozonides of the alkaline earth metals have not been reported.

There are numerous important applications (1) for higher oxides of alkali and alkaline earth metals. In general, these oxides are used as solid source of either activated oxygen or molecular oxygen. Peroxides are widely used for bleaching, the surface treatment of metals, the analysis of refractory ores and oxides, the manufacture of organic peroxides, and the regeneration of air in enclosed environments.

Table 1

Oxides Of Alkali And Alkaline Earth Metals

	Alkali		Alkaline Earth	
	Formula	Member Synthesized	Formula	Member Synthesized
Monoxide	M_2O	Li to Cs	LO	Mg to Ba
Peroxide	M_2O_2	Li to Cs	LO_2	Mg to Ba
Superoxide	MO_2	Na to Cs (Li uncertain)	$L(O_2)_2$	Ca to Ba (low purity)
Ozonide	MO_3	Na to Cs	$L(O_3)_2$	none

Superoxides react with water (vapor or liquid) at ambient temperatures, generating molecular oxygen and alkaline hydroxides which can absorb CO_2 according to the reactions

$$2MO_2\ (s) + H_2O\ (l) = 2MOH\ (s) + 3/2\ O_2\ (g) \qquad (1\text{-}1)$$

$$2MOH\ (s) + CO_2\ (g) = M_2CO_3\ (s) + H_2O\ (l) \qquad (1\text{-}2)$$

Overall:

$$2MO_2\ (s) + CO_2(g) = M_2CO_3\ (s) + 3/2O_2\ (g) \qquad (1\text{-}3)$$

As a result of these reactions a single compound can be used to supply the O_2 necessary for respiration and simultaneously remove the CO_2 given off as a product of respiration. Furthermore because of their strong oxidizing power the superoxides will destroy air-borne bacteria and toxic or noxious materials present in the breathing atmosphere (2,3). As a rsult superoxides are ideally suited for non-regenerative air revitalization in life support systems used for manned space flight and for submarines. It should be noted that potassium superoxide has been used for some time as an emergency source of breathing oxygen for rescue operations in fires and mine accidents and for military first aid.

Although the ozonides could also be conceived of as sources of oxygen their extreme chemical and thermal instability makes them less suitable for this purpose.

The amount of O_2 released and CO_2 scrubbed per pound of superoxide is listed in Table 2 for a number of superoxides. The quantity of each superoxide required to produce 1.87 lbs. of oxygen, which is necessary for respiration per man per day, is also shown in Table 2. The corresponding quantities for Li_2O_2 are also included for comparison.

Of the superoxides KO_2 finds the greatest application because of the relative ease of formation of this compound. However, it would be highly desirable to synthesize other superoxides and in particular those of lithium and calcium. It is seen from Table 2 that LiO_2, if synthesized, would be by far the best of all superoxides in terms of the O_2 available and CO_2 absorbed per pound of superoxide. It would yield 80% more O_2 and absorb 81% more CO_2 than KO_2. Another reason for seeking alternative forms of superoxide is that KO_2 suffers from a low percentage of utilization (about 50%) which imposes a weitht penalty on its use. The reason for the low utilization percentage is that the KOH formed by the reaction of KO_2 with water is hygroscopic and absorbs water forming a

Table 2

Comparison Of O_2 Released And CO_2 Absorbed Using Different Superoxides

	lbs. O_2 Released / lb. Superoxide	lbs. CO_2 Absorbed. / lb. Superoxide	lbs. Superoxide to Generate 1.87 lbs O_2
LiO_2	0.61	0.56	3.03
NaO_2	0.43	0.40	4.28
KO_2	0.34	0.31	5.53
RbO_2	0.20	0.19	9.15
CsO_2	0.15	0.13	12.86
$Ca(O_2)_2$	0.46	0.42	4.03
Li_2O_2	0.35	0.96	5.37

viscous coating around the unused portion of the KO_2 pellet. As a result further water penetration is impeded and the rate of O_2 release is reduced. It is believed that if a nonhygroscopic hydroxide were formed this problem could be avoided. This would certainly be the case for $Ca(O_2)_2$ which would also give 35% more O_2 and absorb 36% more CO_2. Thus $Ca(O_2)_2$, if available, would present two advantages - a higher content of O_2 and a higher potential utilization.

Although a potentially superior material, LiO_2 has not been synthesized so far in high purity. Snow (4) has performed thermodynamic calculations with regard to the stability of LiO_2. While he concludes that LiO_2 is unstable relative to Li_2O or Li_2O_2 this does not preclude the possibility of LiO_2 synthesis, since once formed, LiO_2 may be stable by virtue of the kinetics of decomposition. A variety of methods (1) used to synthesize other superoxides are listed in Table 3. All of these methods except No. 5 have persistently failed to form LiO_2 even in low purity. This conclusion is surprising considering that O_2 pressures as high as 7000 atm. at 200°C have been attempted (1). It has been reported by Vol'nov (1) that the disproportionation of $Li_2O_2 \cdot 2H_2O_2$ gives only 7 to 9% by weight of LiO_2 in an admixture of Li_2O_2,

Table 3

Techniques Used For The Synthesis Of Superoxides

(1) Oxidation of metals dissolved in liquid ammonia

(2) Direct oxidation of metal vapor

(3) Oxidation of a lower oxide

(4) Oxidation of a hydroxide

(5) Disproportionation of peroxide-peroxyhydrate $M_2O_2 \cdot xH_2O_2$

LiOH and LiO_2. It is also claimed by Vol'nov (5) that the reaction of Li_2O_2 with O_3 at low temperature forms LiO_2 identified by EPR measurement. Thus the synthesis of LiO_2 so far is not well established.

It is quite interesting to note that while bulk LiO_2 has not been prepared Andrews (6) and Andrews and Pimentel (7) have demonstrated an interesting approach for forming LiO_2 molecules. In their approach beams of atomic lithium and molecular oxygen were simultaneously impinged on a solid argon matrix. The molecules of LiO_2 thus formed were indentified by infrared spectroscopy. The method while capable of producing single molecules of LiO_2 does not appear to be practical for synthesizing LiO_2 in bulk form.

Attempts to synthesize $Ca(O_2)_2$ in high purity by the conventional techniques listed in Table 3 have all been unsuccessful as has been a recent effort to synthesize $Ca(O_2)_2$ by electrochemical reduction of O_2 to O_2^- in dimethyl sulfoxide and then mixing $CaCl_2$ as the source of calcium ion (8). The use of O_2 pressures as high as 3000 - 4000 atm. at 250°C also does not help to form high purity calcium superoxide (1). While the preparation of pure $Ca(O_2)_2$ has not yet been achieved, several reports have described the formation of this product in an impure form. Thus, Vol'nov (1) has

indicated that vacuum drying of $CaO_2 \cdot 2H_2O_2$ at relatively low temperatures (~50°C) and low pressures (~10 torr) yields $Ca(O_2)_2$ in 55% purity. The starting material, $CaO_2 \cdot 2H_2O_2$ is formed by reacting $CaO_2 \cdot 8H_2O$ with H_2O_2. Petrocelli and Chiarenzelli (9) have also reported preparation of calcium superoxide in 60% purity by the reaction between $Ca(OH)_2$ and H_2O_2. This method has also been recently investigated by Wydeven (10) who obtained maximum purity of 55%. Finally Bosset and Vannerberg (11) have described the preparation of a solid phase containing $Ca(O_2)_2$ with 23% purity by drying $CaO_2 \cdot 8H_2O$ at 100 - 250°C. These authors also studied the crystal structure of the impure material by X-ray diffraction. The X-ray data did not reveal the occurence of a separate phase for $Ca(O_2)_2$. Instead, the lattice was found to consist of a CaO_2 phase, with a CaC_2 structure, in which some of O_2^{2-} ions were statistically replaced by O_2^-, O^{2-} and OH^- ions. Some of the Ca^{+2} ions were also substituted by O_2^- ions. This study suggests that impure preparations of calcium superoxide, which always contain $Ca(OH)_2$ and/or CaO_2 are not likely to contain $Ca(O_2)_2$ as a separate phase, mechanically mixed with CaO_2 and $Ca(OH)_2$. It is quite possible that $Ca(O_2)_2$ is not thermodynamically stable in pure form and that it can

only be stabilized by formation of a solid solution with the lower oxides and hydroxides of calcium.

Since the attempts to synthesize LiO_2 and $Ca(O_2)_2$ in high purity by the conventional synthesis techniques have not been successful, an approach which merits consideration is the use of atomic oxygen or other activated oxygen species formed in an electric discharge. Vol'nov and co-workers (12) have reported the synthesis of higher oxides of sodium, potassium, magnesium, calcium and strontium prepared by subjecting the metal hydroxides to an electric discharge sustained in oxygen. For this work the reactants were placed in the positive column of a direct current discharge at 0.5 torr and 500 watts of discharge power. Table 4 shows a summary of the results, indicating the weight percentages of peroxide and superoxides present in the product. Of particular interest is the observation that 2.2% of $Ca(O_2)_2$ was formed from $Ca(OH)_2$. Similar experiments with LiOH were attempted by Vol'nov but no higher oxides of lithium were obtained.

Hollahan and Wydeven (13) have demonstrated the synthesis of the peroxide and superoxide of rubidium and cesium by subjecting the hydroxides of these metals to the products of a radiofrequency discharge sustained in

Table 4

Summary Of Vol'nov's Results Of Experiments With Hydroxides In A dc Discharge Of Oxygen

Starting Material	Composition Of Product, Wt%		
	Peroxide	Superoxide	Hydroxide
NaOH	31.4	11.4	57.2
KOH	none	80.5	19.5
$Mg(OH)_2$	4.0	none	96.0
$Ca(OH)_2$	47.8	2.2	50.0
$Sr(OH)_2$	46.0	8.0	46.0

oxygen. These authors used a relatively large diameter (3 in) tubular reactor, the flow of oxygen being perpendicular to the axis of the reactor. The reactants were placed directly inside the glow of the discharge. The maximum content of higher oxides in the product expressed in terms of the equivalent weight precent superoxide, which is calculated from the total O_2 released from both peroxide and superoxide, was 54% for the experiments with RbOH and 65% for the experiments with CsOH. For RbOH the maximum conversion was obtained under the condition of 0.5 torr, 50 watts of discharge power and 5 hrs, of reaction time. The corresponding operating conditions for CsOH were 0.5 torr, 70 watts and 3 hrs of reaction time.

The results of Vol'nov and those of Hollahan and Wydeven have clearly established the feasibility of using the products of an oxygen discharge in the synthesis of superoxides. Consequently it was the objective of this work to further explore the method for the synthesis of KO_2 and the possible synthesis of LiO_2 and $Ca(O_2)_2$. In each case synthesis from the pure metal and its hydroxide were considered. As part of this effort the thermodynamics pertaining to reactions between lithium and atomic oxygen and calcium and atomic oxygen were developed. The results were

used to establish the relative stability of the various metal oxides and to interpret the observed experimental results.

CHAPTER 2

THERMODYNAMICS OF SUPEROXIDES OF LITHIUM AND CALCIUM AND FOR REACTIONS OF ATOMIC OXYGEN WITH LITHIUM, LiOH, CALCIUM AND $Ca(OH)_2$

2.I. THERMODYNAMICS OF SUPEROXIDE OF LITHIUM AND FOR REACTIONS OF ATOMIC OXYGEN WITH LITHIUM AND LiOH

2.1.1. Standard Free Energy Of Formation Of LiO_2 As A Function Of Temperature

With only one exception all attempts to synthesize LiO_2 have failed (1). Only in one instance has there been report of successful synthesis of LiO_2 (7-9% by weight obtained by vacuum dessication of $Li_2O_2 \cdot 2H_2O_2$) and there is some doubt about the validity of the report (1). In view of these results it is quite possible that LiO_2 in its pure form is thermodynamically unstable and hence it is important to examine the thermodynamics of LiO_2 and the lower oxides of lithium. Since the properties of pure LiO_2 are not known, the

thermodynamics must be studied theoretically.

A theoretical study of the thermodynamics of LiO_2 has been presented by Snow (4). Based on the knowledge of the crystal structures of other alkali metal (Na, K, Rb, Cs) superoxides, he assumed the structure of LiO_2 to be the same as that of NaCl and calculated the lattice energy using a value of the Madelung constant corresponding to a NaCl-structure (face-centered cubic). The heat of formation $\Delta H^{o}_{f,\ 298}$ for LiO_2 was evaluated using a Born-Haber cycle. To calculate $\Delta F^{o}_{f,T}$ it was assumed that the specific heat for the superoxide is the same as that of NaO_2 and that the standard entropy of LiO_2 can be calculated by Latimer's ion contribution technique (14). The results of Snow's computations are shown in Fig. 1. The corresponding values of $\Delta F^{o}_{f,T}$ for Li_2O_2 and Li_2O taken from the literature are included for the sake of comparison.

D'Orazio and Wood (15) have also investigated the thermodynamics of LiO_2 but in much less detail than Snow. These authors calculated the lattice energies of the superoxides of cesium, rubidium and potassium and then plotted the values against some property (not mentioned) of either the alkali metals or alkali metal superoxides. The lattice energy for LiO_2 was estimated by extrapolation. The standard enthalpy of formation

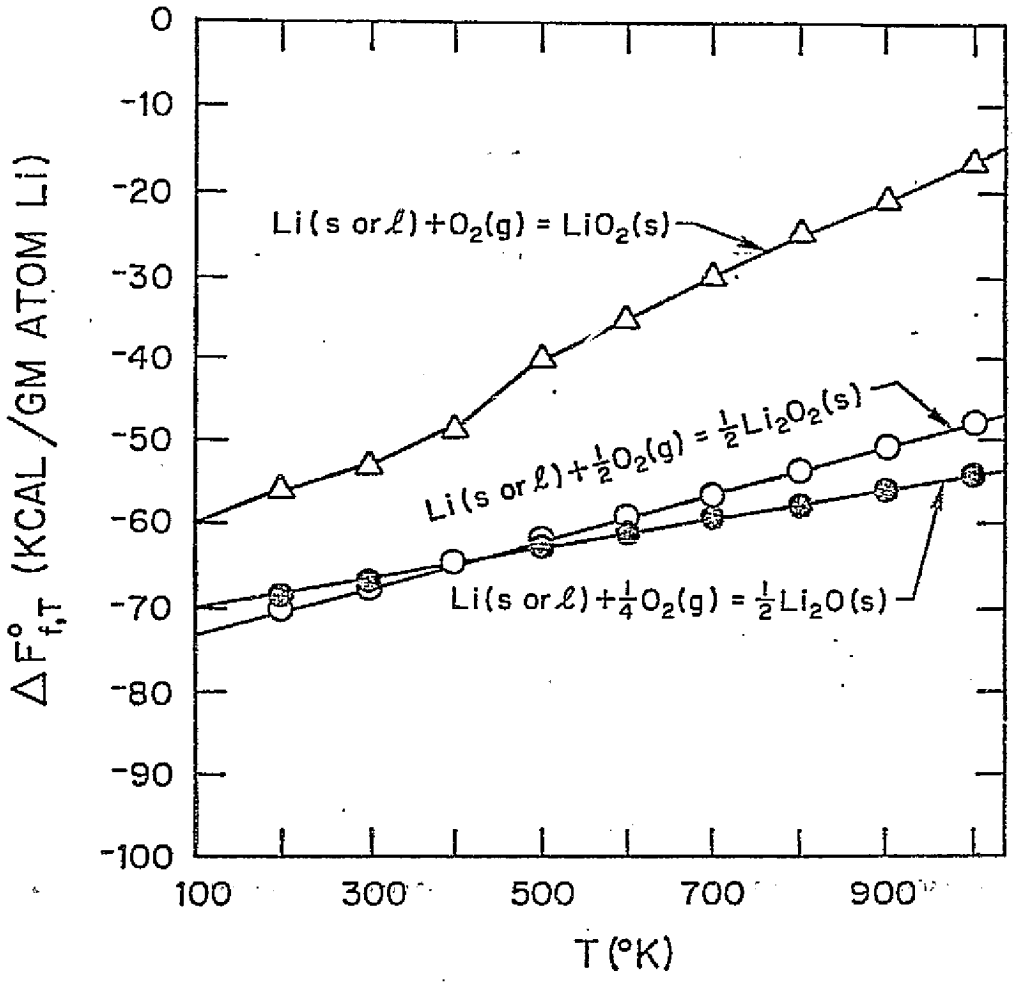

Figure 1. Standard Free Energies of Formation of the Oxides of Lithium as a Function of Temperature

of LiO_2 was estimated by means of a Born-Haber cycle which yielded a value of $\Delta H^{o}_{f} = -62 \pm 10$ kcal/mole. Although the temperature corresponding to the above value of ΔH^{o}_{f} was not mentioned, if it is assumed that the temperature is equal to 298^{o} K then it compares well with Snow's value of -69 kcal/mole at the same temperature.

It is observed in Fig.1 that ΔF^{o}_{f} for LiO_2 in the temperature range 100^{o} - 1000^{o} K is always negative - the magnitude varying from -60 to -17 kcal/mole. However, the values of ΔF^{o}_{f} for Li_2O_2 and Li_2O based on one mole of lithium are much more negative than those for LiO_2. Thus thermodynamically speaking the formation of LiO_2 is feasible but the substance will be unstable with respect to the lower oxides of lithium. This explains the difficulty in synthesizing LiO_2 in pure form.

2.1.2. Standard Free Energy Changes For Reactions Of Atomic Oxygen With Lithium And LiOH

Once the values of $\Delta F^{o}_{f,T}$ for LiO_2, Li_2O_2 and Li_2O are available, the standard free energy changes for the reactions of atomic oxygen with metallic lithium and LiOH to give LiO_2, Li_2O_2 or Li_2O can be estimated easily. In calculation of these values, the thermodynamic data

for lithium, LiOH and atomic oxygen and H_2O were taken from standard references (16, 17, 18). For lithium, LiOH, oxides of lithium and atomic oxygen the standard states were chosen to be the most stable states of the substances at 1 atm and at the temperature under consideration. However, for H_2O the standard state was chosen to be gaseous water at 1 atm at the temperature in question. This selection was made mainly because thermodynamic data for this standard state were easily available.

The results of the calculations indicated are shown in Fig.2. It is observed that for the reaction of atomic oxygen with metallic lithium to give LiO_2 ΔF^o_T is much more negative than the values for similar reactions forming Li_2O_2 or Li_2O. However, this result is not surprising, because the former reaction involves two atoms of oxygen whereas the latter reactions only one or half an atom of oxygen. Since the free energy of formation of atomic oxygen is highly positive, the reaction involving two atoms of oxygen gives the most highly negative value of ΔF^o_T.

Figure 2 indicates that the formation of LiO_2 is thermodynamically feasible in presence of atomic oxygen. One recognizes, however, that if LiO_2 were formed it would still be unstable relative to the lower oxides

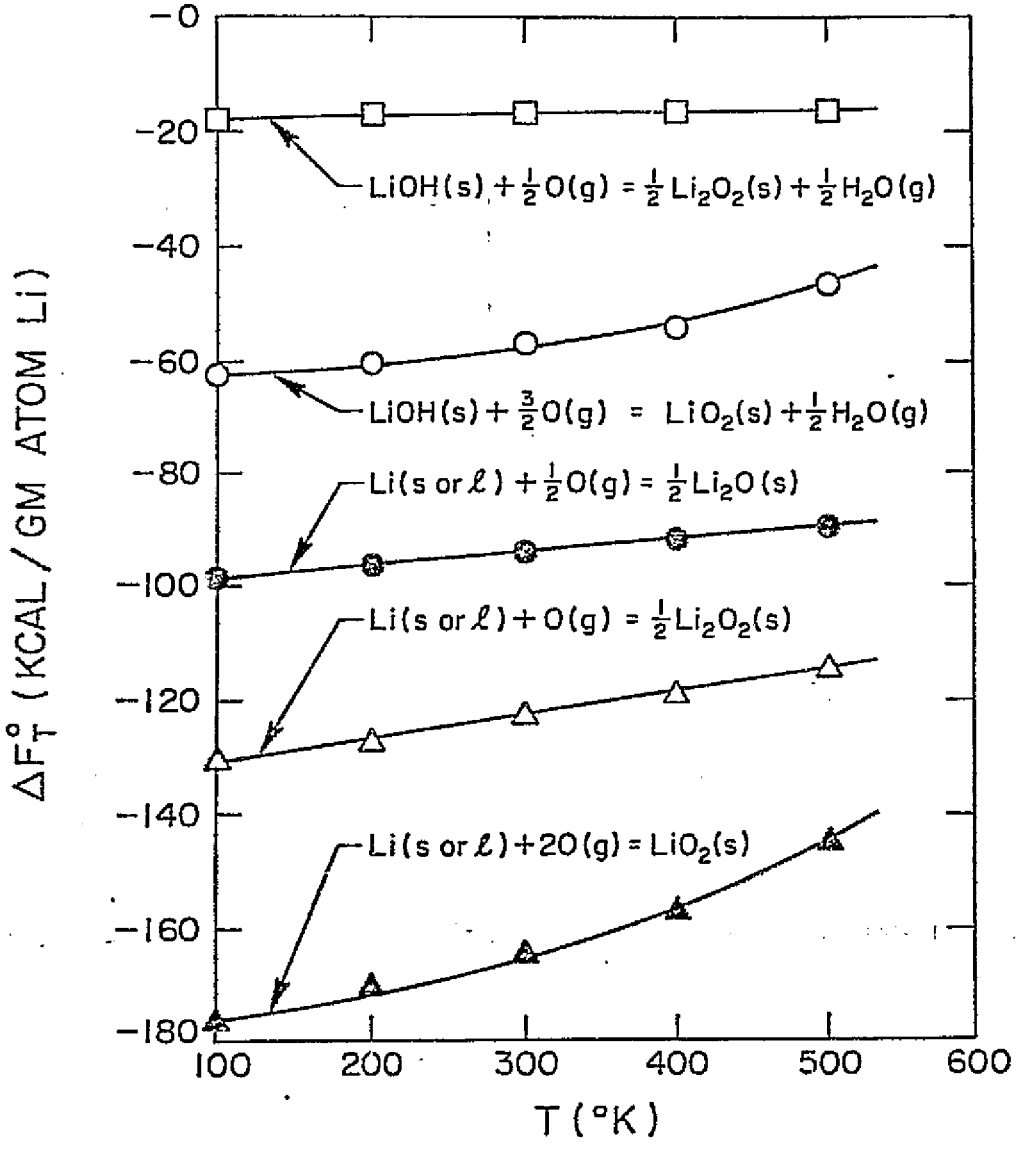

Figure 2. Standard Free Energy Changes for the Reactions of Atomic Oxygen with Metallic Lithium and LiOH

of lithium. Hence it may be possible to prepare LiO_2 but only if the conversion to the lower oxide is hindered by kinetics.

A similar series of calculations were carried out for LiOH as a starting material and the conclusions are exactly the same as for lithium. The corresponding values of ΔF^{o}_{T} are also shown in Fig.2.

2.2. THERMODYNAMICS OF SUPEROXIDE OF CALCIUM AND FOR REACTIONS OF ATOMIC OXYGEN WITH CALCIUM AND $Ca(OH)_2$

2.2.1. Need For Thermodynamics Of $Ca(O_2)_2$

As was discussed in Chapter 1 previous attempts to synthesize $Ca(O_2)_2$ have failed to yield a pure porduct and those reports which do indicate the presence of $Ca(O_2)_2$ in the product relate to a substitutional solid solution which contains O_2^- anions in a matrix of lower oxides. Consequently the thermodynamic properties of $Ca(O_2)_2$ have not been measured experimentally and they must be evaluated theoretically. In this instance there have been no previous investigations. The only reference to this question, appearing in the literature, is a brief comment by Margrave (19) that $Ca(O_2)_2$ is expected to be unstable. No quantitative support for

this conclusion was presented. In view of this a detailed evaluation of the free energy of formation of $Ca(O_2)_2$ was undertaken. The method and results are described in the following sections.

2.2.2. Born-Haber Cycle For $Ca(O_2)_2$

Since $Ca(O_2)_2$ is assumed to be an ionic compound, by analogy with known superoxides, the standard heat of formation can be determined by use of a Born-Haber cycle. The particular cycle chosen is shown below.

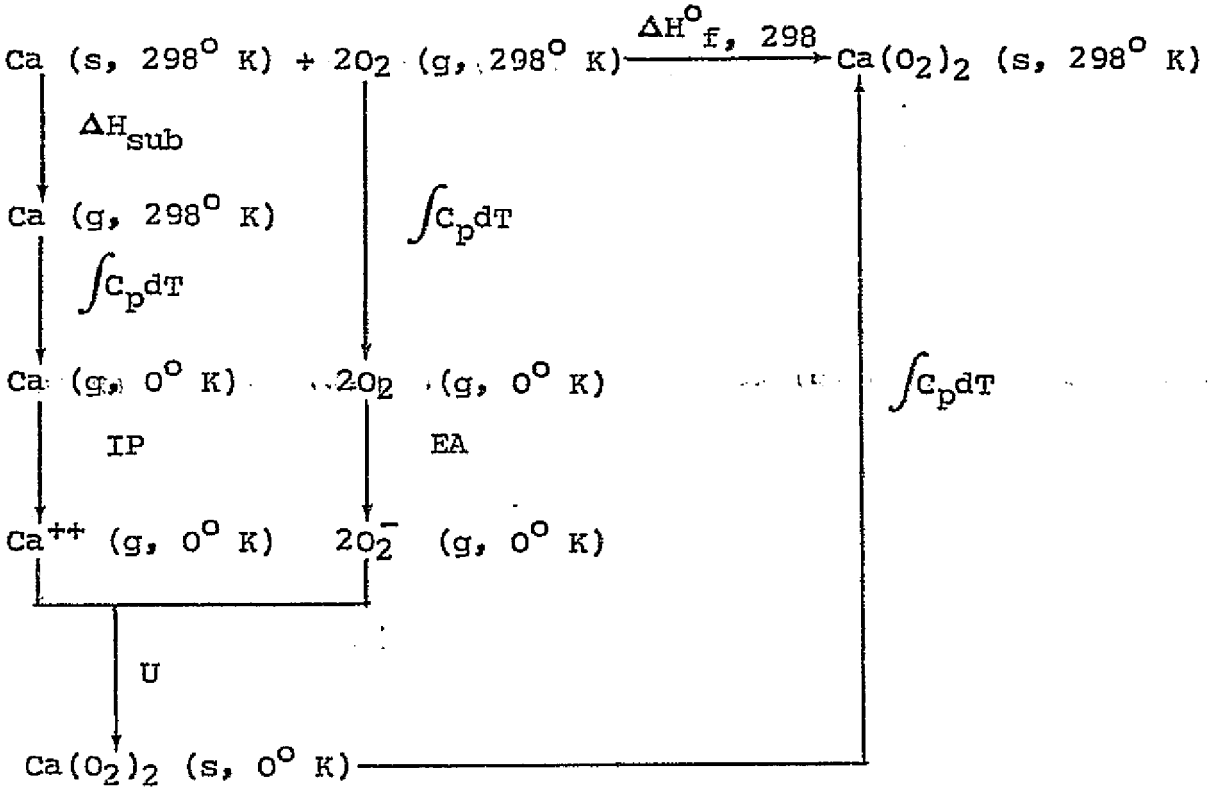

The standard heat of formation of $Ca(O_2)_2$ can be written as the algebraic sum of the energy terms involved in the cycle. Thus

$$\Delta H^{o}_{f,\ 298} = \Delta H_{sub} + \int_{298}^{o} C_{p_{Ca(g)}} dT + IP + 2 \times \int_{298}^{o} C_{p_{O_2(g)}} dT + 2 \times EA + U + \int_{o}^{298} C_{p_{Ca(O_2)_2(s)}} dT \qquad (1)$$

where ΔH_{sub} is the heat of sublimation of calcium at $298^{o}K$, C_p is the molar heat capacity, IP is the ionization potential of calcium, EA is the electron affinity of O_2 and U is the lattice energy of $Ca(O_2)_2$.

It should be noted that except for the lattice energy and the heat capacity of $Ca(O_2)_2$ all other quantities in eqn.1 are properties of elemental calcium and oxygen and as a result are well established. Of the remaining two quantities the lattice energy makes a considerably larger contribution to $\Delta H^{o}_{f,\ 298}$ than does the term containg $C_{p_{Ca(O_2)_2}}$. Consequently, the lattice energy must be evaluated accurately.

2.2.3. Calculation Of Lattice Energy Of $Ca(O_2)_2$

2.2.3.1. Theoretical Consideration

The classical Born-Mayer method can be used to

calculate the lattice energy for ionic solid (20). According to this technique the lattice energy is represented as

$$U = N \cdot \phi(r) \qquad (1a)$$

where N is the Avogadro's number. The potential function $\phi(r)$ gives the energy per molecule as a function of the interionic distance r and is expressed as

$$\phi(r) = -\frac{Me^2}{r} - \frac{C}{r^6} + B(r) + \phi_o \qquad (2)$$

where M is the Madelung constant, e is the electronic charge, C is a constant characteristic of $Ca(O_2)_2$, B(r) is a potential function and ϕ_o is the zero-point energy of $Ca(O_2)_2$. The first term on the right hand side of eqn.2 gives the Coulombic or electrostatic interaction among ions in the lattice, the second term gives the van der Waals interaction energy, the potential function B(r) gives the repulsive energy between the ions. The expression given by Ladd and Lee (21) can be used to represent the repulsive potential B(r)

$$B(r) = b\exp(-r/\rho). \qquad (3)$$

where b is the intensity parameter and ρ is the range parameter. Thus eqn. 2 can be expressed as

$$\phi(r) = -\frac{Me^2}{r} - \frac{C}{r^6} + b\exp(-r/\rho) + \phi_o \qquad (4)$$

To compute $\phi(r)$ we must know all the parameters involved in eqn. 4. However, we can eliminate some of them using properties of the function $\phi(r)$. Thus at the equilibrium interionic distance r_o,

$$\left.\frac{dU}{dr}\right|_{r = r_o} = 0 \qquad (5)$$

$$\text{i.e.,} \quad \left.\frac{d\phi}{dr}\right|_{r = r_o} = 0 \qquad (6)$$

Thus differentiating $\phi(r)$ in eqn. 4 and using eqn. 6,

$$\frac{Me^2}{r_o^2} + \frac{6C}{r_o^7} - \frac{b}{\rho}\exp(-r_o/\rho) = 0 \qquad (7)$$

$$b\exp(-r_o/\rho) = \left[\frac{Me^2}{r_o^2} + \frac{6C}{r_o^7}\right]\rho \qquad (8)$$

So, for an equilibrium interionic distance, r_o, eqn. 4 can be written as

$$\phi(r_o) = -\frac{Me^2}{r_o} - \frac{C}{r_o^6} + \left[\frac{Me^2}{r_o^2} + \frac{6C}{r_o^7}\right]\rho + \phi_o$$

$$= -\frac{Me^2}{r_o}\left[1-\frac{\rho}{r_o}\right] - \frac{C}{r^6{}_o}\left[1-6\frac{\rho}{r_o}\right] + \phi_o \qquad (9)$$

For simple ionic solids the van der Waals term, C/r_o^6, usually corresponds to 1-3% of the lattice energy (22) although calculation by D'Orazio and Wood (15) indicates that this interaction is about 5% of the lattice energy. However, the term ρ/r_o for $Ca(O_2)_2$, as we shall see later, is about 0.13. Thus the term in the second braces of eqn. 9 is 0.22. Hence, the contribution of the second term of eqn. 9 will not be more than about 1% of the lattice energy. Furthermore, the zero-point energy ϕ_o is about 1% or less of the lattice energy and this term is opposite in sign to that of the second term in eqn. 9. So, the combined effect of the last two terms in eqn. 9 is negligibly small compared to the first term. Equation 9 can then be written as

$$\phi(r_o) = -\frac{Me^2}{r_o}\left[1-\frac{\rho}{r_0}\right] \qquad (10)$$

The lattice energy thus becomes

$$U = N\phi(r_o) = - N\frac{Me^2}{r_o}\left[1- \rho/r_o\right] \qquad (11)$$

The application of eqn. 11 will permit evaluation of the lattice energy provided the numerical values of the parameters M, r_o and ρ are known.

2.2.3.2. Evaluation of Madelung Constant, Radius Of Superoxide Ion And Parameter ρ.

The Madelung constant is the sum of a series arising from the expression for the interactions due to Coulombic attraction and repulsion among the ions in the crystal lattice. Evaluation of this sum requires the knowledge of the geometrical arrangement of the ions and the relative distances among the ions in the lattice. Thus to estimate M accurately, the crystal structure must be known. If the crystal structure for which the Madelung constant is to be determined is not known, we may take advantage of the following characteristic of the Madelung constant. If two ionic solids have identical crystal structures and the relative positions of the ions are the same in the two lattices, then both crystals will have the same Madelung constant (22). Thus if the crystal structure of the solid we are interested in is not known experimentally but can be established from other available information, we can take the Madelung

constant for the solid to be the same as that of a crystal which has the same structure.

If the ions in the lattice are spherically symmetric then the position of the charge can be identified as being located at the center of the sphere. For non-spherical ions, such as the superoxide anion (O_2^-), it is no longer correct to assume the net charge of the ions to be concentrated at its center. Accurate calculation of the Madelung constant in such cases requires that the charge distribution on the non-spherical ions be known or assumed. D'Orazio and Wood (15) have calculated the Madelung constants for potassium, rubidium, and cesium superoxides both by assuming the superoxide ion to be spherical as well as non-spherical, taking a charge distribution of $-\frac{1}{2}e$ per oxygen atom. It was found, however, that the lattice energies calculated from the two values of the Madelung constant differed only by 2% for KO_2 and by less than 2% for RbO_2 and CsO_2. Based on these results it was assumed that the O_2^- anion could safely be assumed to be spherically symmetric for the present calculations of the lattice energy.

The first step in determining the Madelung constant for $Ca(O_2)_2$ is to establish the crystal structure of the solid. A useful guide for this purpose is the ratio of anion to cation radii, r_a/r_c. The numerical value of this ratio indicates the possible structure

the solid might possess (22, 23). Thus it is necessary to estimate the radius of the superoxide anion, r_a, to establish the possible structure of $Ca(O_2)_2$. A numerical value of this radius is also necessary to calculate the lattice energy U from eqn. 11, since r_o, the inter-ionic distance, is taken to be the sum of the radii of the cation and anion. This is, of course, tantamount to the assumption that the ions touch each other and indeed, this assumption is part of the model adopted to calculate the ionic radii by Pauling and others (23, 24).

The radius of the superoxide ion can be estimated from the consideration of the properties of NaO_2 in the following way. In case of NaO_2, $\Delta H^o_{f,\ 298}$ has been estimated experimentally. So the lattice energy for NaO_2 can be calculated using the known value of $\Delta H^o_{f,\ 298}$ and a Born-Haber cycle. Once the lattice energy is evaluated application of eqn. 11 will permit the evaluation of r_o provided the Madelung constant and ρ are known. The crystal structure of NaO_2 has been determined by x-ray diffraction (25). It has a face-centered cubic structure which is stable at room temperature and is represented as NaO_2 (I). Thus the Madelung constant for NaO_2 (I) can be taken to be the same as that of NaCl which also has a face-centered cubic

Structure. The parameter ρ is the only remaining quantity which must be estimated before attempt is made to calculate r_o and hence r_a for $O_2^{=}$.

The range parameter ρ is usually evaluated from the experimentally determined bulk modulus of the crystal. The bulk modulus is defined as

$$\text{B.M.} = 1/ - \frac{1}{V}\frac{dV}{dP}$$

$$= -V\frac{dP}{dV} \qquad (12)$$

where V is the volume of the solid, P is the applied pressure. From thermodynamics

$$dU = TdS - PdV$$

where S is the entropy of the solid. At T=0

$$dU = - PdV$$

or $$\frac{d^2U}{dV^2} = - \frac{dP}{dV}$$

Hence eqn. 12 may be written as

$$\text{B.M.} = V\frac{d^2U}{dV^2} \qquad (13)$$

The quantity d^2U/dV^2 can be related to ϕ by eqn. 1a, so that

$$\frac{d^2U}{dV^2} = N\left[\frac{d\phi}{dr}\,\frac{d^2\phi}{dV^2} + \frac{d^2\phi}{dr^2}\left(\frac{dr}{dV}\right)^2\right] \tag{14}$$

At the equilibrium interionic distance r_o,

$$\frac{d\phi}{dr} = 0\,, \qquad V = V_o$$

and hence

$$\left.\frac{d^2U}{dV^2}\right|_{V = V_o} = N\left[\frac{d^2\phi}{dr^2}\left(\frac{dr}{dV}\right)^2\right]_{r = r_o} \tag{15}$$

Referring to eqn. 13 we see that

$$\left.\frac{d^2U}{dV^2}\right|_{V = V_o} = \frac{B.M.}{V_o} \tag{16}$$

Thus eqn. 14 can be written as

$$N\left[\frac{d^2\phi}{dr^2}\left(\frac{dr}{dv}\right)^2\right]_{r = r_o} = \frac{B.M.}{V_o} \tag{17}$$

If the crystal structure of the solid is known, the

relationship between r and V can be determined easily and hence dr/dV can be estimated. Since $d^2\phi/dV^2$ depends upon ρ, this parameter can be determined provided the bulk modulus is known. Fortunately, the values of ρ calculated for simpler crystals do not vary more than 2-3%. Thus ρ for NaO_2 (I) as well as for $Ca(O_2)_2$ can be assumed to be the same as that of the alkali halides (26).

Since the Madelung constant, M, for NaO_2 (I) and the parameter ρ have been evaluated, the ionic radius of O_2^- can now be estimated from the lattice energy for NaO_2 (I). The lattice energy is determined by using the Born-Haber cycle shown below together with the measured value of $\Delta H^o_{f,\ 298}$.

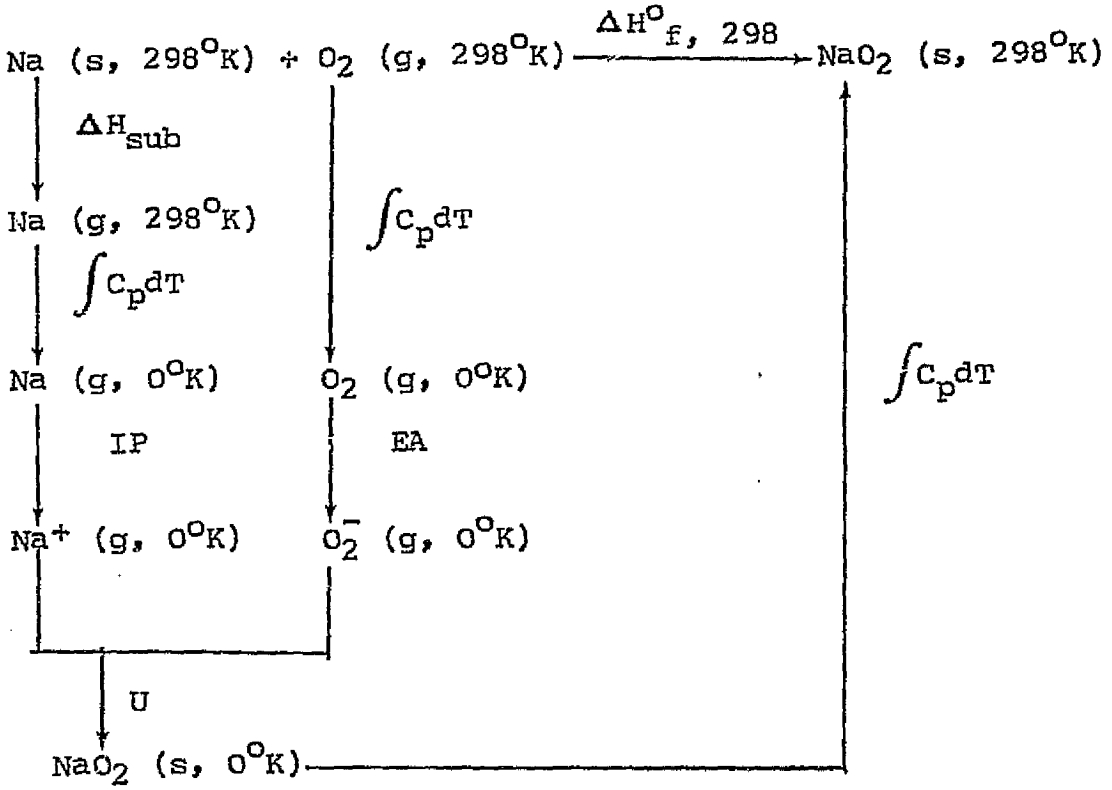

$$\text{Thus } U = \Delta H^{\circ}_{f,\,298} - \left[\Delta H_{sub} + \int_{298}^{0} C_{p_{Na(g)}} dT + IP + \int_{298}^{0} C_{p_{O_2(g)}} dT + EA + \int_{0}^{298} C_{p_{NaO_2(s)}} dT \right] \qquad (18)$$

Once U is known r_o can be determined from eqn. 11

$$U = -\frac{Me^2}{r_o}\left[1 - \frac{\rho}{r_o}\right] \qquad (11)$$

The data needed to evaluate U and r_o for NaO_2 (I) are given in Table 5. The lattice energy for NaO_2 (I) and

Table 5. Data Required To Calculate U And r_o For $NaO_2(I)$

Property	Numerical Value	Reference
ΔH_{sub} for Na	26.3 kcal/mole	29
IP for Na	118.5 kcal/mole	45
EA for O_2	-10.1 kcal/mole	45
$\int_{298}^{o} C_{p_{Na(g)}} dT$	-1.5 kcal/mole	*
$\int_{298}^{o} C_{p_{O_2(g)}} dT$	-2.1 kcal/mole	49
$\int_{o}^{298} C_{p_{NaO_2(s)}} dT$	3.9 kcal/mole	15, 30
$\Delta H^{o}_{f,\ 298}$ for $NaO_2(I)$	-62.5 kcal/mole	49
Madelung const. for $NaO_2(I)$	1.747	22, b

Table 5 (Continued)

Property	Numerical Value	Reference
ρ for NaO_2	0.32 Å	15, 26
r_c for Na^+	0.95 Å	22

* calculated assuming ideal gas value of $C_p = 5/2R$
a taken to be the same as that for KO_2
b see text

the interionic distance are -197.5 kcal/mole and 2.59 Å respectively. From the determined value of r_o it is possible to conclude that r_a for the O_2^- anion is 1.64 Å.

2.2.3.3. Numerical Estimation Of The Lattice Energy Of $Ca(O_2)_2$

Once the value of the anion radius, r_a, is known a possible structure for $Ca(O_2)_2$ can be determined. Evaluation of the ratio r_a/r_c for $Ca(O_2)_2$ gives

$$\frac{r_a}{r_c} = \frac{1.64}{0.97} = 1.69$$

This ratio suggests (22) that $Ca(O_2)_2$ is likely to have a rutile crystal lattice in which each cation is surrounded octahedrally by six anions and each anion is surrounded by three cations in a triangular fashion. From the considerations of the most stable packing of the ions in the lattice it has been shown that if the radius ratio, r_a/r_c, for an AB_2 type ionic solid lies between 1.37 and 2.44, then the structure is likely to be the same as that of rutile (22).

Based upon the conclusion that the lattice structure of $Ca(O_2)_2$ is the same as that for rutile it may now be concluded further that the Madelung constant for $Ca(O_2)_2$ is the same as that for rutile. The Madelung constant for rutile has been determined by a number of workers (27, 28). For the present work the value given by Johnson and Templeton (28) was used to determine

the lattice energy of $Ca(O_2)_2$ by means of eqn. 11. The data used in this calculation and their sources are given in Table 6. The lattice energy for $Ca(O_2)_2$ obtained from eqn. 11 is -532.2 kcal/mole. Introducing this value of the lattice energy into eqn. 1 gives $\Delta H^{o}_{f,\ 298}$ = -94.4 kcal/mole.

Table 6. Data Required to Calculate U and $\Delta H^{o}_{f,298}$ for $Ca(O_2)_2$.

Property	Numerical Value	Reference
ΔH_{sub} for Ca at 298°K	40.3 kcal/mole	16
IP for Ca $\rightarrow$ Ca^{++}	414.5 kcal/mole	45
EA for O_2	-10.1 kcal/mole	45
$\int_{298}^{o} C_{p_{Ca(g)}} dT$	-1.5 kcal/mole	*
$\int_{298}^{o} C_{p_{O_2(g)}} dT$	-2.1 kcal/mole	49
$\int_{o}^{298} C_{p_{Ca(O_2)_2}} dT$	8.9 kcal/mole	a
Madelung constant for $Ca(O_2)_2$	4.79	28
r_a for O_2^-	1.64 Å	b
ρ for $Ca(O_2)_2$	0.32 Å	15, 26

Table 6 (Continued)

Property	Numerical Value	Reference
r_c for Ca^{++}	0.97 Å	22
ΔC_p for reaction (2-1)	6.0 cal/(^oC)(mole)	b
Entropy contribution of each O_2^- in $Ca(O_2)_2$	19.4 e.u.	14, b
Entropy contribution of Ca^{++} in $Ca(O_2)_2$	9.3 e.u.	14

---

* calculated from assumption of ideal gas $C_p = 5/2R$

a calculated from Dulong and Petit rule and assuming C_p to be constant over the temp. range

b see text

2.2.4. Standard Free Energy Of Formation Of $Ca(O_2)_2$ As A Fuction Of Temperature

The standard free energy of formation, $\Delta F^{o}_{f,\ T}$, for $Ca(O_2)_2$ at different temperatures can now be estimated by the following procedure. The reaction under consideration is

$$Ca\ (s,\ T) + 2O_2\ (g,\ T) = Ca(O_2)_2\ (s,\ T) \qquad (2\text{-}1)$$

For this reaction

$$\Delta F^{o}_{f,\ T} = \Delta H^{o}_{f,\ T} - T\Delta S^{o}_{f,\ T}$$

$$= \Delta H^{o}_{f,\ 298} + \int_{298}^{T} \Delta C_p dT - T\left[\Delta S^{o}_{f,\ 298} + \int_{298}^{T} \frac{\Delta C_p dT}{T}\right] \qquad (19)$$

where $\Delta H^{o}_{f,\ T}$ is the standard heat of formation of $Ca(O_2)_2$ at temperature T, $\Delta S^{o}_{f,\ T}$ is the standard entropy change for formation of $Ca(O_2)_2$ at temperature T and ΔC_p is the difference in heat capacities. Application of eqn. 19 requires a knowledge of the standard entropy change of formation of $Ca(O_2)_2$ at 25°C and the value of ΔC_p as a function of temperature. Since $Ca(O_2)_2$ has not been synthesized in pure form the specific heat and absolute entropy at standard conditions for this substance must

be estimated theoretically.

An approximate guide for estimating C_p for unknown solids involving gaseous reactants has been given by Kubaschewski, Evans and Alcock (29). For a reaction such as

$$A\,(s) + xB_2\,(g) = AB_{2x}\,(s) \qquad (2\text{-}2)$$

$$\Delta C_p = C_{p_{AB_{2x}(s)}} - C_{p_{A(s)}} - x \cdot C_{p_{B_2(g)}}$$

$$= 3x \text{ cal}/(^{o}C)(\text{mole}) \qquad (20)$$

This method of calculating ΔC_p may be contrasted with the one in which the specific heats of each compoment are evaluated seperately. Thus, according to Dulong & Petit's rule (29) the molar heat capacity of a solid element is 6 cal/(^{o}C)(g. atom) and that of a solid compound is six times the number of atoms in the stoichiometric formula of the solid. From the kinetic theory of gases the heat capacity of diatomic molecules is known to be 7 cal/(^{o}C)(mole). Thus, the approximate value of ΔC_p for the above reaction should be

$$\Delta C_p = (2x + 1)\ \ 6 - 6 - 7x$$

$$= 5x \qquad (21)$$

It has been found, however, that the experimentally determined values of ΔC_p are closer to 3x than to 5x for many solid reactions involving gaseous reactants. In the case of $NaO_2(s)$ eqn. 20 yields a value of ΔC_p which is within 20% of the value calculated from experimentally determined specific heats for $NaO_2(s)$, $Na(s)$, and $O_2(g)$ at 25°C. For KO_2 the calculated value of ΔC_p differs by 50% from that determined using the experimental specific heats. The effect of a 50% error in ΔC_p is to introduce an error of 8% in the C_p for $KO_2(s)$ if it is calculated from ΔC_p and the C_p of $K(s)$ and $O_2(g)$. It is anticipated that a similar level of error should hold for $Ca(O_2)_2(s)$.

As a further assumption ΔC_p for $Ca(O_2)_2$ is considered to be constant between 160° and 500°K. This assumption is based on the following observations. Over the specified temperature range, the specific heat of oxygen varies by only 6% while that for calcium by less than 3%. Thus the variation in the specific heat of $Ca(O_2)_2$ should be no more than a few percent. Such a conclusion is found to be valid for NaO_2 and KO_2 (30). Furthermore evaluation of the term containing ΔC_p indicates that it contributes no more than 2 to 3% to the magnitude of $\Delta H^o_{f,\,298}$.

Calculation of $\Delta S^o_{f,\,298}$ requires that $S^o_{Ca(O_2)_2}$

at 298°K, be known. This quantity must also be determined theoretically. For this purpose Latimer's ion contribution technique (14) may be used. This procedure states that for ionic solids the entropy at 298°K can be evaluated by a summation of the contributions from the cation and anion. Since the entropies of NaO_2 and KO_2 at 298°K are known from experimentally determined values of C_p, the contribution for O_2^- can be calculated by subtracting the contribution due to Na^+ and K^+ respectively. Contributions due to O_2^- calculated for these two superoxides differ by 7.5%. An arithmatic mean of the two values was taken for the calculation of $S^o_{Ca(O_2)_2}$ at 298°K. No further correction was made to this figure to account for the higher valence of Ca^{++} relative to Na^+ or K^+. The entropy contribution of Ca^{++} was taken from Latimer's calculation (14) and the entropies of Ca(s) and O_2(g) from standard references (16, 17). All of the data used to calculate $S^o_{Ca(O_2)_2}$ are given in Table 6. The final value of $\Delta S^o_{f,\ 298}$ obtained by this procedure is -58.37 e.u.

Standard free energies of formation for $Ca(O_2)_2$, calculated at different temperatures by the procedure described above are plotted in Fig. 3. Similar quantities for CaO and CaO_2 are also plotted in the same figure. Free energies for these two oxides were taken from the

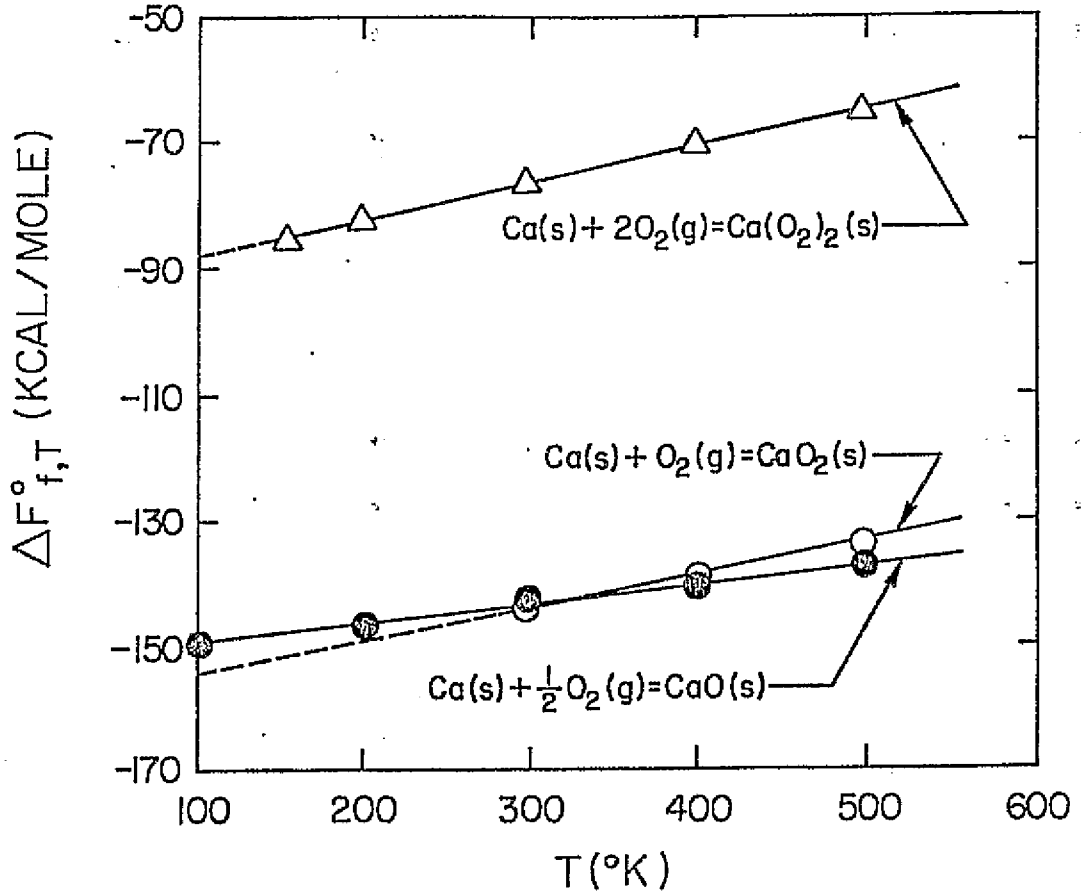

Figure 3. Standard Free Energies of Formation of the Oxides of Calcium as a Function of Temperature

literature (16, 31). For CaO_2 the standard free energy of formation was not available for temperatures below 298.16°K. Below this temperature standard free energy was linearly exptrapolated (dotted line).

It is observed that $\Delta F^{o}_{f,\ T}$ for $Ca(O_2)_2$ is highly negative for the entire temperature range considered in the present work. However, the values of $\Delta F^{o}_{f,\ T}$ for CaO or CaO_2 are even more negative than that for $Ca(O_2)_2$ over the same temperature range. For example at room temperature $\Delta F^{o}_{f,\ T}$ for $Ca(O_2)_2$ is about 65 kcal less negative than the values for CaO or CaO_2. Corresponding differences at other temperatures are of similar magnitude. This means that the thermodynamic driving force for conversion of $Ca(O_2)_2$ to CaO and CaO_2 is extremely large. Thus, even if $Ca(O_2)_2$ were formed it would decompose to CaO or CaO_2 unless it was kinetically stable. This observation could explain the repeated failure to synthesize pure $Ca(O_2)_2$ under a variety of conditions.

2.2.5. Standard Free Energy Change For Reactions Of Atomic Oxygen With Calcium And $Ca(OH)_2$

Once $\Delta F^{o}_{f,\ T}$ for $Ca(O_2)_2$ are known ΔF^{o}_{T} for reactions of atomic oxygen with elemental calcium and $Ca(OH)_2$ leading to $Ca(O_2)_2$ can easily be undertaken. Values

of ΔF_T^o for such reactions are shown in Fig. 4. For completeness the values of ΔF_T^o for similar reactions leading to CaO_2 and CaO are also included in Fig. 4. In these calculations the thermodynamic data for calcium, $Ca(OH)_2$, CaO, CaO_2, atomic oxygen and H_2O were taken from standard references (16, 17, 31). For calcium, oxides of calcium, $Ca(OH)_2$ and atomic oxygen the standard states were chosen to be the most stable states of the substances at 1 atm. and at the temperature under consideration. However, for H_2O the standard state was chosen to be gaseous water at 1 atm independent of the temperature. This selection was made mainly because thermodynamic data with this standard state were easily available. It is seen that of three reactions between solid calcium and atomic oxygen the one leading to $Ca(O_2)_2$ has the largest negative standard free energy change. However, this is not surprising since the stoichiometry of the reaction leading to $Ca(O_2)_2$ from solid Ca requires four atoms of oxygen, which are associated with a large positive free energy change relative to molecular oxygen. For the same reason the ΔF_T^o for the reaction giving CaO_2 from solid calcium is much more negative than that for the reaction leading to CaO. Although these reactions indicate that formation of $Ca(O_2)_2$ is thermodynamically possible in the presence of

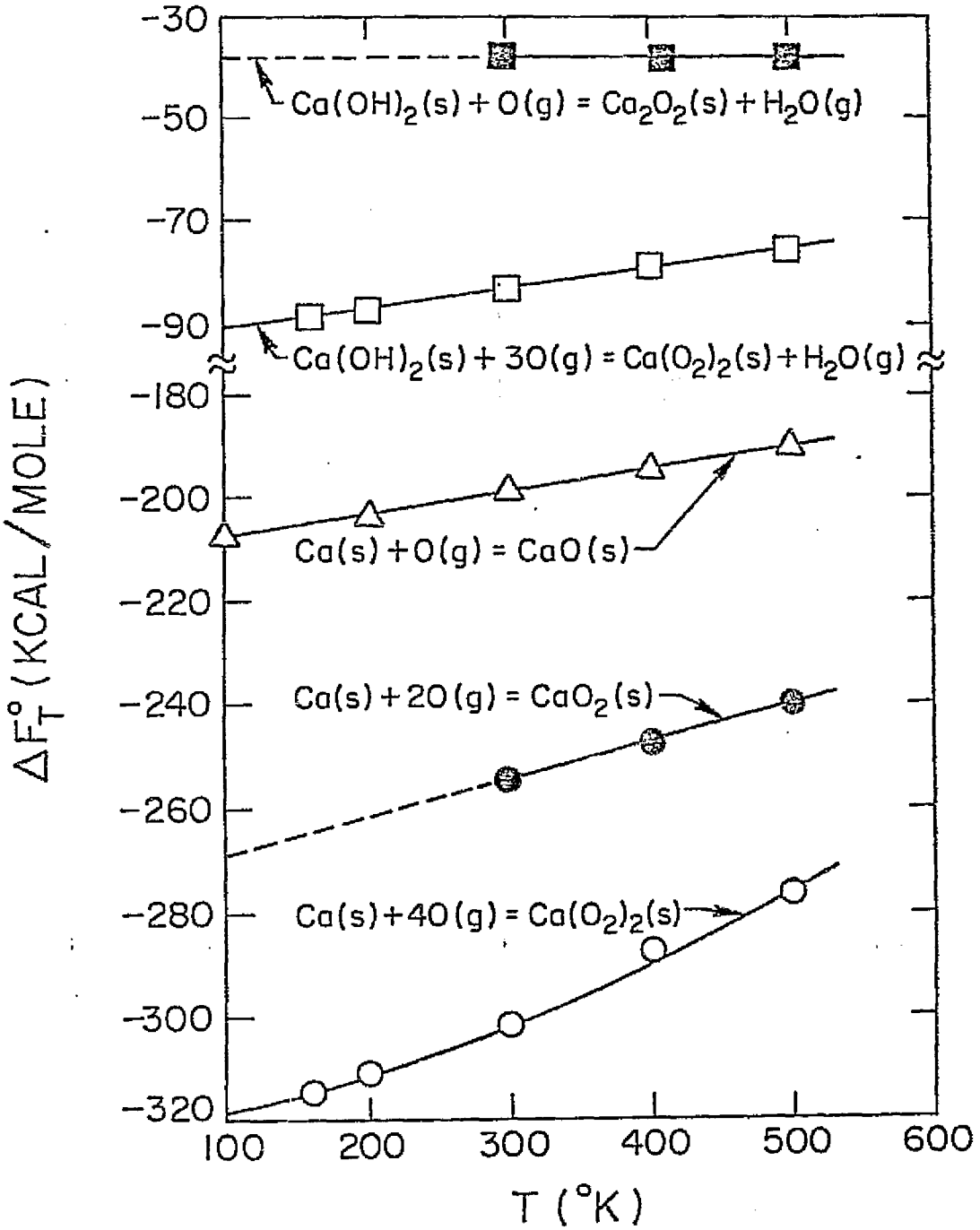

Figure 4. Standard Free Energy Changes for the Reactions of Atomic Oxygen with Metallic Calcium and $Ca(OH)_2$

atomic oxygen, the instability of $Ca(O_2)_2$ with respect to the lower oxides, shown in Fig. 3, still holds there and one is led to the conclusion that while it may be possible to form $Ca(O_2)_2$ it would not be stable unless its rate of conversion to the lower oxides were quite low. Similar conclusions can be drawn with regard to using $Ca(OH)_2$ as the source of calcium as shown by the results in Fig. 4.

A further result which can be deduced from the thermodynamics presented here is as follows. Inspection of Fig. 3 reveals that the free energies of formation of CaO_2 and CaO are nearly the same, the former being slightly larger above 300°K and the latter slightly larger below 300°K. Because of the small driving force for conversion of CaO_2 to CaO it is expected that CaO_2 should be a relatively stable product. As will be discussed in Chapter 4 CaO_2 can in fact be prepared from $Ca(OH)_2$ subjected to discharged oxygen.

CHAPTER 3

EXPERIMENTAL APPARATUS AND PROCEDURE

3.1. APPARATUS AND PROCEDURE FOR EXPERIMENTS WITH ELEMENTAL POTASSIUM,LITHIUM AND CALCIUM

3.1.1. Apparatus For Experiments With Elemental Potassium, Lithium And Calcium

The apparatus used for investigating the reactions of elemental potassium, lithium, and calcium with discharged oxygen is shown in Fig. 5. The discharge reactor consists of a quartz tube (14" long x 1¼" i.d.) with a side tube (6" long) at its center. The ends of the discharge tube are made of pyrex glass and are joined to the central quartz section by graded seals.

A miniature furnace introduced through the side tube was used to generate metal vapor. The furnace consists of a cylindrical block heated by a 70W cartridge heater (Superwatt, model Hotwatt 2126) which was fitted into a hole (1½" long x ¼" dia.) drilled in the block. The insulated lead wires from the heater are taken out through a stainless steel tube welded

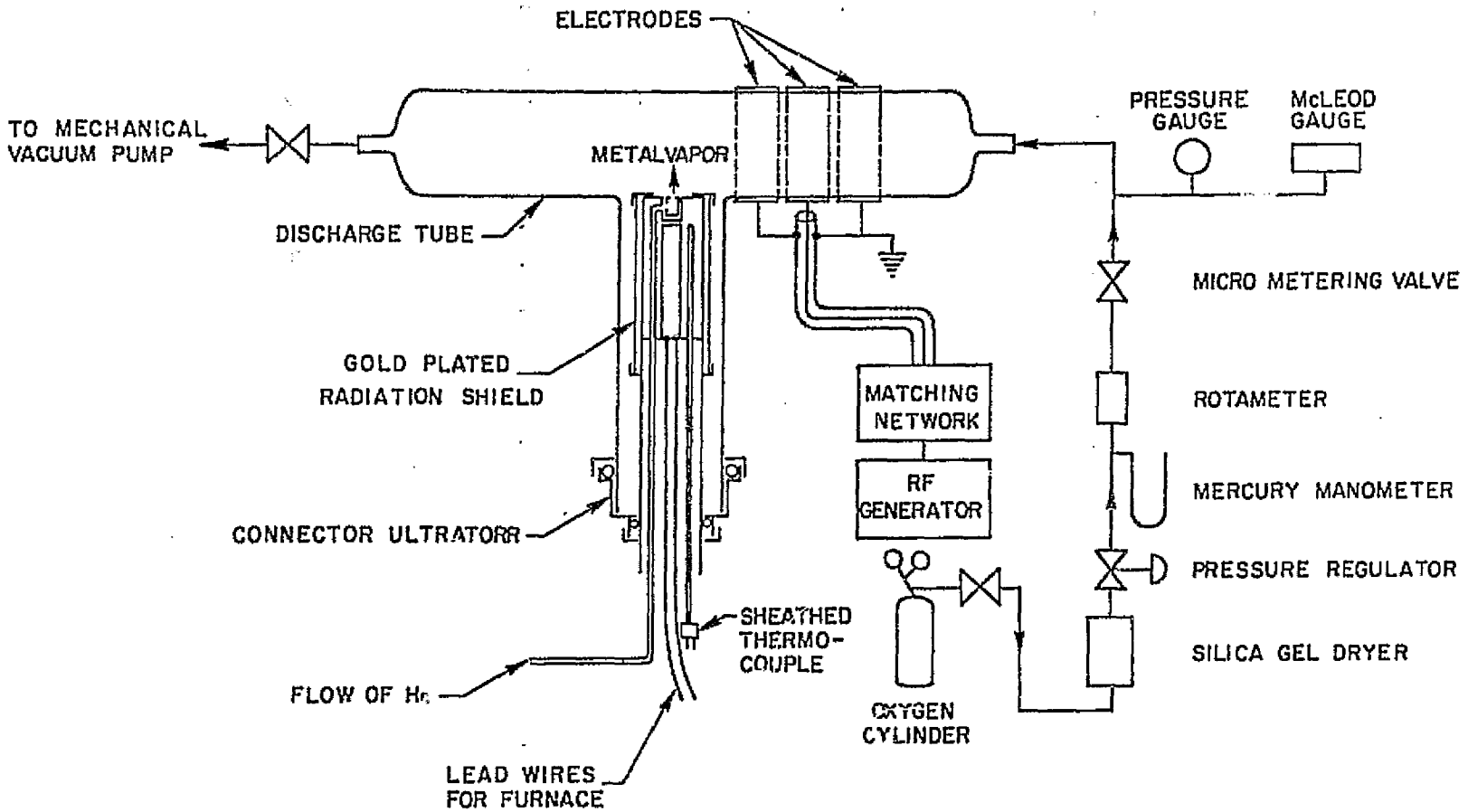

Figure 5. Schematic Diagram of the Apparatus for Experiments With Metal Vapors

to the nickel block. A hole at the top of the block holds a monel cup (5/16" long x 1/4" dia.) containing the metal to be evaporated. The contents of the cup could be blanketed with helium fed through a 1/16" passage drilled into the nickel block. The temperature of the block is measured with a sheathed chromel-alumel thermocouple (Thermo-Electric ISA - K) connected to a potentiometer.

The nickel block is welded to a stainless steel tube of the same diameter which acts as a support for the block. Three concentric stainless steel radiation shields mounted on a grooved collar are used to reduce heat losses from the furnace. A grooved lid was used to cover the top of the radiation shields. The radiation shields were plated with gold to reduce their emissivity for radiation. However, most of the gold evaporated after heating the furnace to a high temperature a few times. With the radiation shields in place the furnace was capable of attaining 750 ^{o}C.

The discharge tube is connected at one end to a flow system which supplies oxygen and at the other end to a mechanical vacuum pump. Oxygen from a cylinder is first dried by passage through a silica gel dryer and then reduced in pressure to slightly above 1 atm by a low delivery pressure regulator (Conoflow, Hammel Dahl,

H 10XT, 0-5). The flow is then metered into the evacuated reactor through a fine metering valve (Whitey SS, 22RS4). The flow rate of oxygen is measured by a microrotameter. Pressure within the reactor is determined by an absolute pressure gauge (Wallace and Tiernan FA 160 - PP12780) or by a McLeod gauge (Gilmont C-333). The power to the discharge is supplied through three ring-shaped copper electrodes mounted on the outside of the discharge tube. The electrodes are coupled to a radiofrequency generator (Tracerlab RFG-600) via an impedance matching network (Tracerlab PA1-600). The generator operates at a frequency of 13.56 MHZ and can deliver up to 350 watts. The power dissipated in the discharge is measured by a power meter located within the generator.

3.1.2. Procedure For Experiments With Elemental Potassium, Lithium And Calcium

The experimental procedure used in the experiments with metallic potassium, lithium and calcium was essentially the same. Pieces of the metal usually stored under a light oil were transferred to a glass trough filled with hexane. In the case of potassium small chips of the metal were cut from a bigger stick under hexane using a sharp knife. The lithium and calcium were available in the form of small beads. In all three cases the

small pieces of the metal were transferred under hexane to the monel cup. The cup now containing the metal and hexane was placed into the nickel block of the furnace. As soon as the furnace was in place the discharge tube was evacuated. Once the hexane was pumped off, the furnace was turned on and allowed to approach the desired temperature. When the temperature was close to the desired value a small flow (a few ml/min) of helium was introduced into the furnace chamber. At this point the oxygen flow was initiated and the pressure set to the desired level. The discharge was then initiated by turning on the generator.

3.2. APPARATUS AND PROCEDURE FOR EXPERIMENTS WITH METAL HYDROXIDES

3.2.1. Apparatus For Experiments With Metal Hydroxides.

The discharge tube used for the reactions between metal hydroxides and discharged oxygen is shown is Fig 6. This tube is of the same size as that used for the studies with metal vapors and is made up of two halves connected by a standard ground glass joint. Stopcocks located at the ends of the tube allow it to be isolated from the flow and vacuum systems and transferred without contamination with the atmosphere.

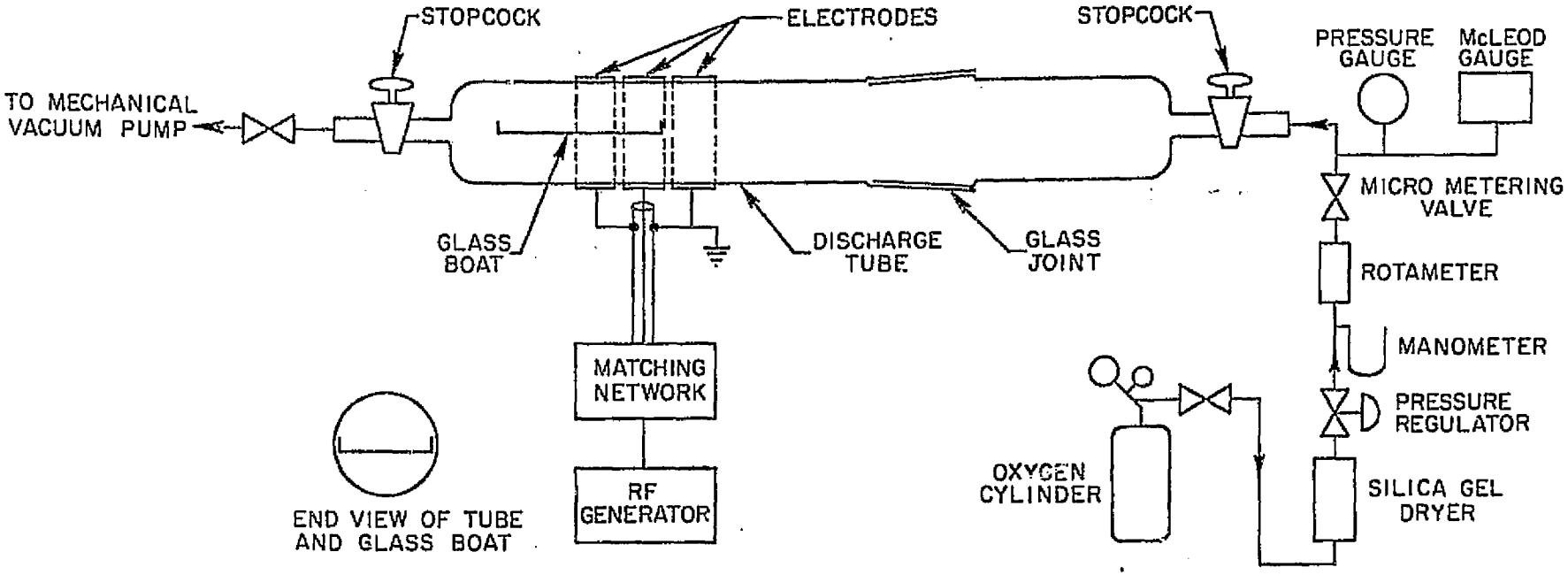

Figure 6. Schematic Diagram of the Apparatus for Experiments with Metal Hydroxides

3.2.2. Procedure For Experiments With KOH, LiOH And $Ca(OH)_2$

For the experiments in which a metal hydroxide was used as the starting material it was found highly desirable to use the hydroxide in the form of a very fine powder. In the cases of KOH and LiOH this was achieved by grinding large particles of these reagents in a mortar and pestle. This operation was carried out in a dry box purged with nitrogen. A half hour of grinding was required for KOH but only 15 minutes for LiOH. $Ca(OH)_2$ was obtained in the form of a very fine powder so that further size reduction was not required.

At the start of each experiment a portion of the finely divided hydroxide was measured using a small ceramic spoon and spread out on the bottom of a flat glass boat (3 3/16" x 1 1/16") in as thin a layer as possible. The boat was then inserted into the discharge tube and isolated by turning the stopcocks to their closed position. At this point the tube was taken from the dry box, connected to the flow system, and evacuated. A flow of oxygen was then established and the run initiated.

3.3. PRINCIPLE, APPARATUS AND PROCEDURE FOR CHEMICAL ANALYSIS OF A MIXTURE OF HIGHER OXIDES

3.3.1. Principle Of Analysis Of A Mixture Of Superoxide And Peroxide

As mentioned in Chapter 1, superoxides react with water according to reaction (1-1). However, the reaction (1-1) takes place in two steps as follows.

$$2MO_2 + 2H_2O = 2MOH + H_2O_2 + O_2 \qquad (3\text{-}1)$$

$$H_2O_2 = H_2O + \tfrac{1}{2}O_2 \qquad (3\text{-}2)$$

The amount of superoxide can thus be determined by measuring the volume of O_2 evolved after complete decomposition of MO_2 according to reactions (3-1) and (3-2). However, it should be noted that superoxides usually contain a certain proportion of peroxides and that the peroxides will also liberate H_2O_2 due to reaction with water via reaction (3-3)

$$M_2O_2 + 2H_2O = H_2O_2 + 2MOH \qquad (3\text{-}3)$$

The H_2O_2 thus formed also decomposes according to reaction (3-2). Although reaction (3-2) is much slower than reaction (3-1) the decomposition of H_2O_2 must be

suppressed in order to obtain an accurate measure of the quantity of superoxide present in a sample containing both superoxide and peroxide.

A technique to suppress reaction (3-2) was first suggested by Seyb and Kleinberg (32) and their method was followed for the work presented here. According to this technique acetic acid diluted with an inert organic solvent reacts with the superoxide liberating O_2:

$$2MO_2 + 2HAc = 2MAc + H_2O_2 + O_2 \qquad (3\text{-}4)$$

The peroxide, if present, forms H_2O_2 by the reaction

$$M_2O_2 + 2HAc = 2MAc + H_2O_2 \qquad (3\text{-}5)$$

By carrying out the reactions at 0^o C the decomposition of H_2O_2 is found to be negligible(33). After measuring the amount of O_2 released by the acetic acid the H_2O_2 is decomposed by adding a $FeCl_3$ solution which acts as a catalyst in the decomposition:

$$H_2O_2 \xrightarrow{FeCl_3} H_2O + \tfrac{1}{2}O_2 \qquad (3\text{-}6)$$

The amount of O_2 evolved by reaction (3-4) corresponds to the amount of superoxide present in the sample being analysed, while the O_2 released by reaction (3-6) corresponds to the total amount of H_2O_2 present in the

solution. The H_2O_2 generated from superoxide is determined by the stoichiometry of reaction (3-4). Hence, the peroxide originally present in the sample can be calculated by difference from the total.

3.3.2. Apparatus For Analysis Of A Mixture Of Superoxide And Peroxide

The apparatus used for analysis of a superoxide - peroxide mixture is shown in Fig. 7. It consists of a small (~40 ml) conical glass reactor which is attached to the system by a ground glass joint. A small graduated buret is attached at the top of the reactor and is used to introduce measured quantities of the solutions required for analysis. A second buret connected to the reactor using a capillary tube is used to measure the volume of O_2 evolved. A mercury reservoir attached to this buret permits adjustment of the gas pressure inside the reactor to the desired level. A small diameter tube is also connected to the second buret to facilitate the comparison of the inside pressure with that of the atmosphere.

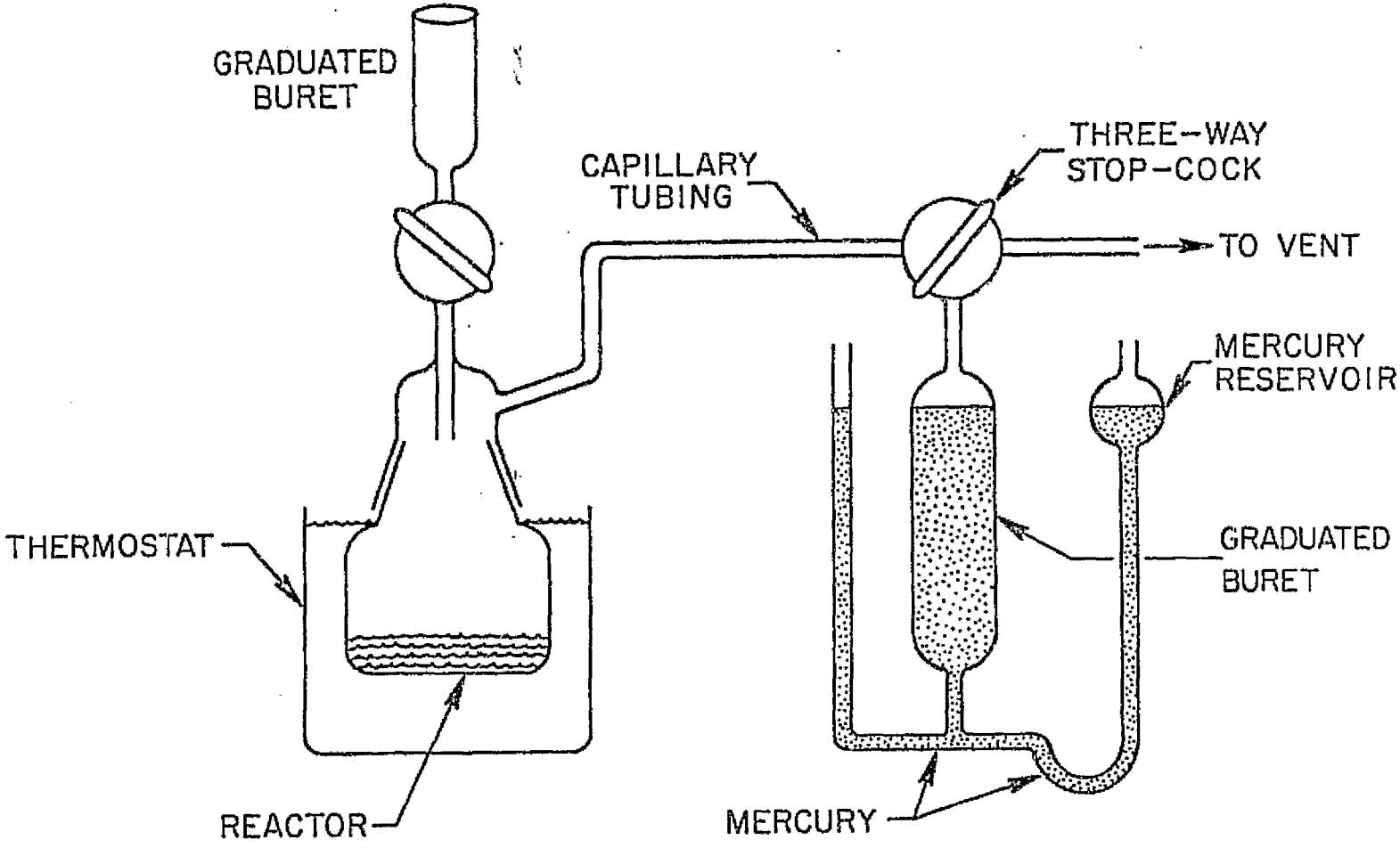

Figure 7. Schematic Diagram for Analysis of Mixtures of Superoxide and Peroxide

3.3.3. Procedure For Analysis Of A Mixture Of Superoxide And Peroxide

To analyze a sample the following procedure was used. The discharge tube containing the reaction product in the boat was opened in a dry box purged continuously with N_2, a portion of the product was scraped from the boat and mixed thoroughly in a mortar and pestle. In the case of experiments with KOH only the yellowest portion of the product was taken for analysis. The material or a portion (10-100 mg) thereof was placed into the clean reactor which was previously weighed with a ground glass lid on it. The reactor was then closed using the same lid and weighed again. Next the lid was removed and the reactor was quickly attached to the balance of the apparatus.

To determine accurately the volume of the O_2 evolved it is necessary to take into account the changes of the enclosed gas volume due to changes of the ambient temperature during the analysis. The gas volume enclosed after attaching the reactor could be easily estimated provided the inside volume upto the beginning of the graduation of the buret was known. To measure this volume the nercury column was first adjusted to equalize the inside pressure to that of the atmosphere and the height of the mercury column was recorded. The inside

pressure was then reduced by a few centimeters of mercury and the volume at the reduced pressure was measured. From these two measurements the enclosed volume up to the beginning of the graduation of the buret was calculated. The volume of the enclosed gas at a particular pressure after attaching the reactor was the sum of the above volume and the buret reading at that pressure.

After the above measurement, a measured quantity (~1.5ml) of diethyl phthalate was introduced into the reactor from the buret, and the reaction was cooled down to 0^{o} C using an ice-water bath. A measured quantity (1.5 - 2 ml) of acetic acid diluted with diethyl phthalate (4:1 V/V) was then slowly added into the reactor. If any superoxide was present in the sample a slow release of O_2 was observed. The completion of the reaction usually took about 1-2 hours depending upon the amount of superoxide present. After the reaction was completed the ice-water bath was removed and the system was allowed to warm up to room temperature and the volume of the gas inside the apparatus was measured. At this point a known quantity (2 - 3 ml) of a solution 3M in $FeCl_3$ and 1M in HCl was added to the reactor. The decomposition of H_2O_2 could be observed in the form of evolution of tiny bubbles. The decomposition was usually slow and hence was allowed to continue overnight.

After the completion of the reaction, the volume of the gas inside the apparatus was measured to estimate the O_2 evolved during the second step. Each measurement of the gas volume inside the apparatus was conducted after equalizing the inside pressure to that of the atmosphere. Also, during each measurement the ambient temperature was recorded to take into account the change in gas volume due to a change in the ambient temperature.

After each complete analysis the amounts of superoxide and peroxide in the sample analyzed were calculated using the following expressions

$$\text{Percent superoxide in the sample} = \frac{M_s \times V_1 \times 100}{22.4 \times 10^3 \times X_1 \times m}$$

$$\text{Percent peroxide in the sample} = \frac{M_p \times V_2 \times 100}{22.4 \times 10^3 \times X_2 \times m}$$

where M_s and M_p are the molecular weights of the superoxide and peroxide respectively, X_1 is the number of moles of O_2 available due to decomposition of superoxide to peroxide, X_2 is the number of moles of O_2 available due to decomposition of peroxide to monoxide or hydroxide, V_1 and V_2 are the volumes of O_2 at STP released during the first and second steps of analysis

respectively, and m is the mass of the sample taken for analysis.

3.4. THERMAL ANALYSIS OF MIXTURE OF SUPEROXIDE AND PEROXIDE OF POTASSIUM

3.4.1. Introduction

During the course of the present work it was observed that Seyb and Kleinberg's wet chemical technique of determining superoxide in a superoxide-peroxide mixture was not always reliable. A similar conclusion has also been reported by Hollahan and Wydeven (13). As a result it was decided to investigate the possibility of using thermogravimetric analysis (TGA) as a means for determining the amount of KO_2 present in a KO_2 - K_2O_2 mixture. It was anticipated that this type of analysis would reveal the thermal behavior of the oxides of potassium and the nature of the chemical interactions among these oxides.

3.4.2. Apparatus And Procedure For Thermal Analysis Of A Mixture Of Superoxide And Peroxide Of Potassium

Thermogravimetric analyses of KO_2 samples prepared commercially and the samples prepared in the course of the present work were performed by a commercial service (Wext Coast Technical Service Inc., Cerritos, CA.). The first analysis, TGA 1, of the

commercial sample was carried out in a thermogravimetric analyzer (Voland and Sons, N. Y.) in which the furnace was continuously purged by flowing helium at a rate of 2-3 cu. ft./hr. at 1 atm. The heating rate was 4-6^{o}C/min. The second analysis, TGA 2, of the same batch of commercial KO_2 and the analyses TGA 3 and 4, of the samples prepared in the present work were performed in an argon atmosphere using a DuPont 950 TG Analyzer. The flow rate of argon was maintained at 0.7 cu. ft./hr and the heating rate was 15^{o}C/min for TGA 2 and 7.5^{o}C/min for TGA 3 and 4. Maintenance of an inert environment during the thermal analyses was very important because of hygroscopicity of KO_2. The first analysis TGA 1 was conducted up to 700^{o}C while the last three analyses, TGA 2 to 4, up to 1100^{o}C.

The differential thermal analyses (DTA) of the commercial sample and the sample used in TGA 4 was performed using a DuPont 900 DT Analyzer. Alumina was chosen as the reference material. The heating rate of the furnace was maintained at about 10-15^{o}C/min, while argon was used to maintain an inert environment in the furnace.

CHAPTER 4

OBSERVATIONS, RESULTS AND DISCUSSION

4.1. OBSERVATIONS AND RESULTS FOR EXPERIMENTS WITH ELEMENTAL POTASSIUM, LITHIUM AND CALCIUM

4.1.1. Experiments With Elemental Potassium

For the experiments with potassium the furnace temperature was maintained at 350°C. At this temperature the vapor pressure of the metal is 0.3 torr. Under these conditions a rich, blue-brown deposit of potassium was observed on the glass wall immediately above the top of the furnace. In some experiments this deposit quickly disappeared, while in others it turned to a yellow-white color as the discharge continued. At some spots on the deposit the color was distinctly yellow. In one experiment a fairly intense yellow color was observed on the lid covering the top of the radiation shields. In yet another experiment the pieces of potassium metal inside the cup turned to an intense, almost canary yellow color.

To get a qualitative indication of the chemical nature of the deposit, it was allowed to react with a small amount of water. This reaction led to the release of a gas. Since any unreacted potassium would have been oxidized rapidly upon exposure of the reactor contents to the atmosphere, it is believed that the observed reaction was that between water and potassium superoxide. Thus the release of gas upon reaction with water and the presence of a yellow product suggest that a small amount of potassium superoxide is formed when potassium vapor reacts with the products of an oxygen discharge.

4.1.2. Experiments With Elemental Lithium

For the experiment with metallic lithium the furnace temperature was set at 720°C to produce a lithium vapor pressure of 1 torr. A deposit similar to that produced by potassium was observed with lithium. However, the color of the deposit was brown, and turned white as the discharge continued. No yellow color was observed. The deposit was allowed to react with water, but no effervescence was observed. Based on this evidence it would appear that no significant amount of superoxide was formed.

4.1.3. Experiments With Elemental Calcium

In case of calcium the furnace was operated at 720°C. At this temperature the vapor pressure of the metal is 0.22 torr. No deposit of solid product was observed on the tube wall, possibly because of the low vapor pressure of calcium. Consequently, to provide more direct contact of elemental calcium and discharged oxygen several pieces of calcium metal were placed in the horizontal section of the discharge tube but to the left of the heater. No change in color of the pieces was observed while the discharge was on. The metal pieces were then placed very close to the center electrode. The pieces immediately adjacent to the electrode turned black. On continuing the discharge for about 25 minutes the black color changed to brown-white. Immediately after the discharge was turned off the brown-white color turned light yellow in about 5-6 seconds. Some of the pieces located a short distance from the central electrode were completely white.

The reacted pieces of metal were allowed to react with distilled water. An initially slow reaction was followed by a rapid reaction between unreacted calcium and water. From these observation no conclusion could be drawn about the possible formation of calcium superoxide.

4.2. RESULTS AND DISCUSSION FOR EXPERIMENTS WITH METAL HYDROXIDES

4.2.1. Exiperiments With KOH

In the early experiments with KOH the discharge electrodes were so positioned that the boat was completely inside the glow of the discharge. Within about 5 minutes or even less the material appeared to "melt", the pressure rose by 20-30% and then the "molten" material solidified gradually forming a thin crust at the top. This crust slowly, but not uniformly, became yellow in color. During this phase of the reaction blister -like formations were observed at the top of the crust. Working in a dry box, a portion of the crust was scraped off with a knife and subjected to analysis. These results show that the product contained only 5-12% of KO_2 by weight. No definite pattern of change in yield with changes in the operating variables was observed for these experiments. This was partly because while scraping out the top layer it was difficult to avoid some unconverted material from the bottom also being scraped and mixed with the sample taken for analysis. The low yield of KO_2 together with the observation that only the crust at the top of the KOH "melt" was characterized by a yellow color suggest that the reaction

of KOH is limited by the formation of the crust which acts as a diffusion barrier.

In the next series of experiments the electrodes were positioned in such a fashion that half of the boat was inside the glow of the discharge and half outside. This arrangement allowed only the material which was inside the glow region to "melt". However, a gradual spread of the "melted" zone was observed so that it finally covered 2/3 of the boat. The entire "molten" zone slowly solidified and formed a thin crust as described above. The particles of KOH, which were closest to the "molten" zone became yellow and the yellow zone slowly moved downstream from the glow region.

In the course of the initial runs it was observed that the particles of KOH were not uniform in size and that the coarser particles in the region outside the glow were not as strongly yellow in color as the small ones. To examine the effects of particle size another series of experiments was performed using more finely ground KOH. The effect of the particle size on the conversion of KOH to higher oxides is indicated in Table 7. The total available O_2 and the weight percent of superoxide obtained with the finer particles are about 3 times greater than those obtained with relatively course particles. Although the reaction time for the

Table 7

Effect Of Particle Size On The Conversion Of KOH To Higher Oxides

Serial No.	Particle Size	Pressure (torr)	Flowrate Of O_2 (ml(STP)/min)	Reaction Time (hr)	Power (watt)	Total O_2 Released From Product (ml(STP)/gm)	Wt.% KO_2 Based On O_2 Released At First Step	Equivalent Wt.% KO_2 Based On Total O_2
1.	Coarse Grit	0.95	2.78	3	70	22.1	7.1	9.3
2.	Powder	0.95	2.78	3	70	66.0	19.7	27.9
3.	Powder	0.96	2.78	4	70	56.7	22.2	23.9

experiment No. 3 in Table 7 is longer it has been observed both in this work and by Hollahan and Wydeven (13) that the effect of time on conversion is marginal after about 3 hrs. Thus the increased yields for experiment No. 2 and 3 compared to that in No. 1 can be attributed to smaller particle size.

Although a higher yield of product could be obtained through the use of fine particles, it was suspected that only the outer crust of these particles had reacted. To test this hypothesis the next series of experiments was carried out in two steps. The particles of KOH were first subjected to the action of the discharge for 3 hrs following the procedure described above. The yellow portion of the material in the boat was then scraped out, reground, spread on half of the boat, and the reaction started again, keeping the material outside the glow. During this second step the material turned more yellow in most of the experiments, indicating a higher conversion to KO_2. The results of such two-step experiments are shown in Fig. 8. The total reaction time for all these reactions was 6 hours - 3 hours for each of the two steps.

Both the pressure and the oxygen flow rate have a strong influence on the conversion of KOH to higher oxides as shown in Fig. 8. At a given flow rate of O_2

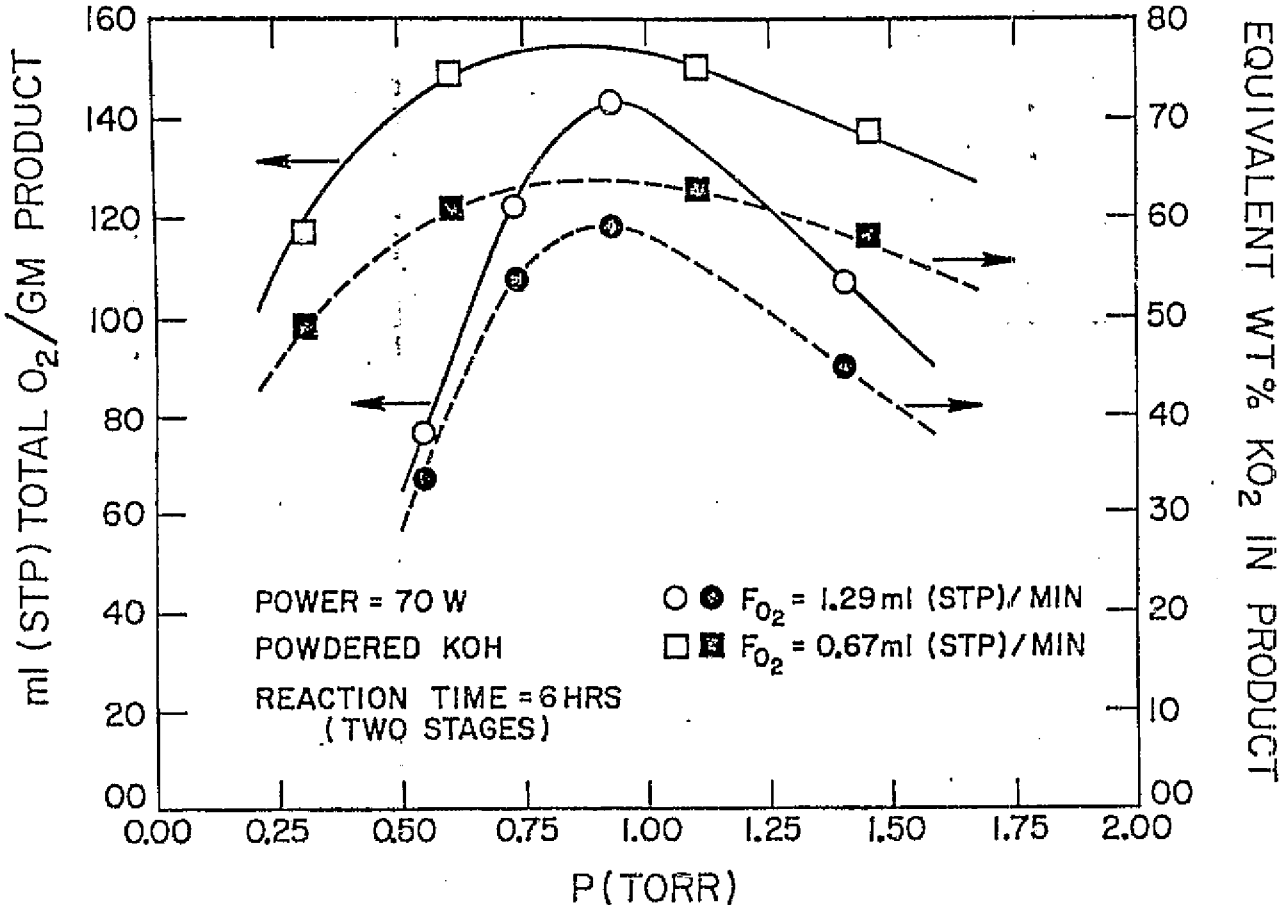

Figure 8. Total Available O_2 and Equivalent Weight Percent KO_2 vs. Discharge Pressure for KOH as the Initial Reactant

the total amount of O_2 available from the product increases with pressure, passes through a maximum and then decreases with further increase in the discharge pressure. At a lower flow rate the conversion increases in most of the experiments. For both the flow rates shown in Fig. 8 the maximum conversion takes place between 0.75 to 1.00 torr. Since the equivalent weight percent of KO_2 has been calculated from the total available O_2 the shapes of the two curves for any given flow rate are very similar.

The effect of power on the conversion of KOH to higher oxides is shown in Fig. 9. The total available oxygen and hence the equivalent weight percent of KO_2 increases with increasing power, passes through a maxium and then decreases with further increase of discharge power. For the experiment at 90W almost all the material in the boat appeared to "melt" and form a thin crust which, as discussed above, is not favorable for high conversion. The reaction time for the experiment carried out at 70W and represented in Fig. 9 is half of that for the experiment with similar operating conditions represented in Fig. 8. The conversion in the former experiment is about 20% higher than that in the latter. It should be noted, however, that the starting material for the two series of experiments, of which these two

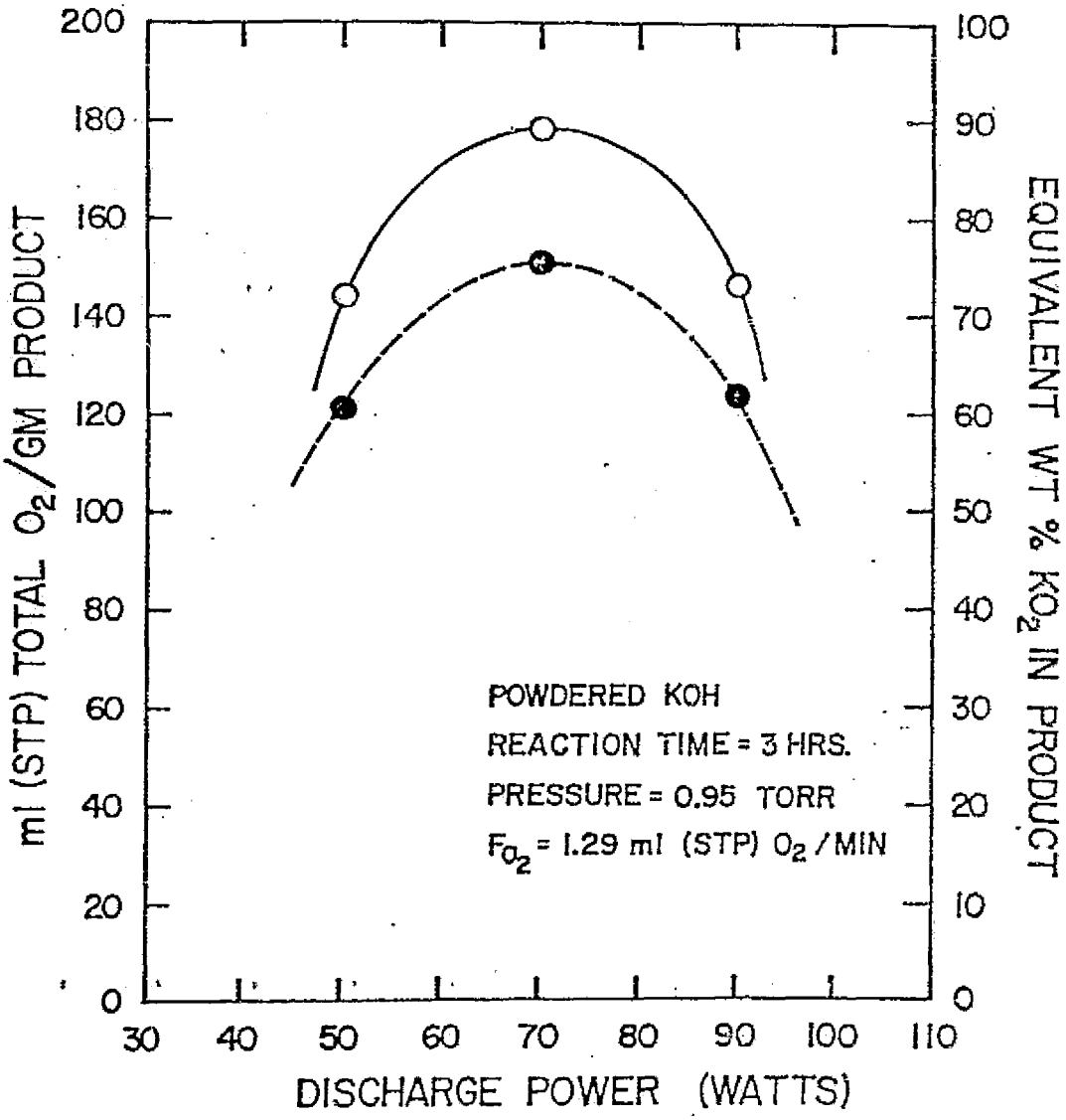

Figure 9. Total Available O_2 and Equivalent Weight Percent KO_2 vs. Discharge Power for KOH as the Initial Reactant

are members was not taken from the same batch of powdered KOH. As a result the average particle size for the two experiments may not have been the same. This difference undoubtedly contributes to part of the observed disagreement.

It should be observed that in Figs. 8 and 9 the weight percent of KO_2 equivalent to the total O_2 released by the product has been calculated instead of the absolute weight percent of KO_2, which is a more desirable quantity. The reason for doing this is as follows. The total O_2 available from the product includes all the oxygen from KO_2 as well as that from the K_2O_2, which is usually present in the product. The absolute weight percent KO_2 can be calculated from the amount of O_2 evolved at the first step of chemical analysis as represented by the stoichiometry of reaction (3-1). This calculation assumes negligible decomposition of H_2O_2 released from the superoxide or the metal peroxide. If no K_2O_2 is present and no decomposition of the H_2O_2 occurs at the first stage, the volume of O_2 at the second step would be exactly half of that at the first stage. The presence of free K_2O_2 would make the volume of O_2 evolved at the second step more than half of that at the first step. The comparison of the relative amounts of O_2 evolved in the two steps for some analyses indicates decomposition

of H_2O_2 during the first steps. In such cases accurate estimate of the absolute amount of KO_2 in the product is not possible. However, there is an indication (33) that decomposition of H_2O_2 at the first step of analysis may not be considerable. Thus an approximate estimate of the weight percent of KO_2 can be obtained by calculating the quantity based on O_2 evolved at the first step, provided the decomposition of H_2O_2 is not considerable. In such cases the difference between the weight percent of KO_2 and the equivalent weight percent of KO_2 is a rough measure of the amount of K_2O_2 present in the product. Thus for the experiment No. 3 in Table 7 this difference is about 9%, indicating a relatively small amount of K_2O_2 in the product. This behavior is also apparent from the observation of the relative amount of O_2 evolved at the two steps of the analysis (see Table A-1, Appendix A). It was observed that for all the experiments corresponding to the higher flow rate of O_2 shown on Fig. 8 the equivalent weight percent of KO_2 and the absolute weight percent of KO_2 are within 2% of each other, an indication of a negligible amount of K_2O_2 in the product.

The explanation for the observations mentioned above is that the conversion to a higher oxide takes place only with the material on the surface of the KOH

particles. Under the conditions of this series of experiments with relatively long reaction time (6 hrs.) all the KOH on the surface was converted to KO_2 which is thermodynamically speaking, the most stable oxide of potassium. The material below the surface layer remains in completely converted to K_2O_2 which is possibly the intermediate in the formation of KO_2 from KOH. This trend has also been observed for most of the experiments with lower flow rates as well as for experiments with discharge power as the independent variable but to a lesser extent.

4.2.2. Experiments With LiOH

During the experiments with LiOH no "melting" or increase of pressure was observed and the product for analysis was taken from the portion of the material which was inside the glow. Also since the particles of LiOH appeared to be finer than those of KOH the effect of intermediate grinding on the conversion was not investigated.

Fig. 10 shows the results from the experiments with LiOH. As mentioned previously, for LiOH there is no formation of LiO_2, although Li_2O_2 is formed in large concentration. This observation can be explained in terms of the thermodynamic properties of the oxides of

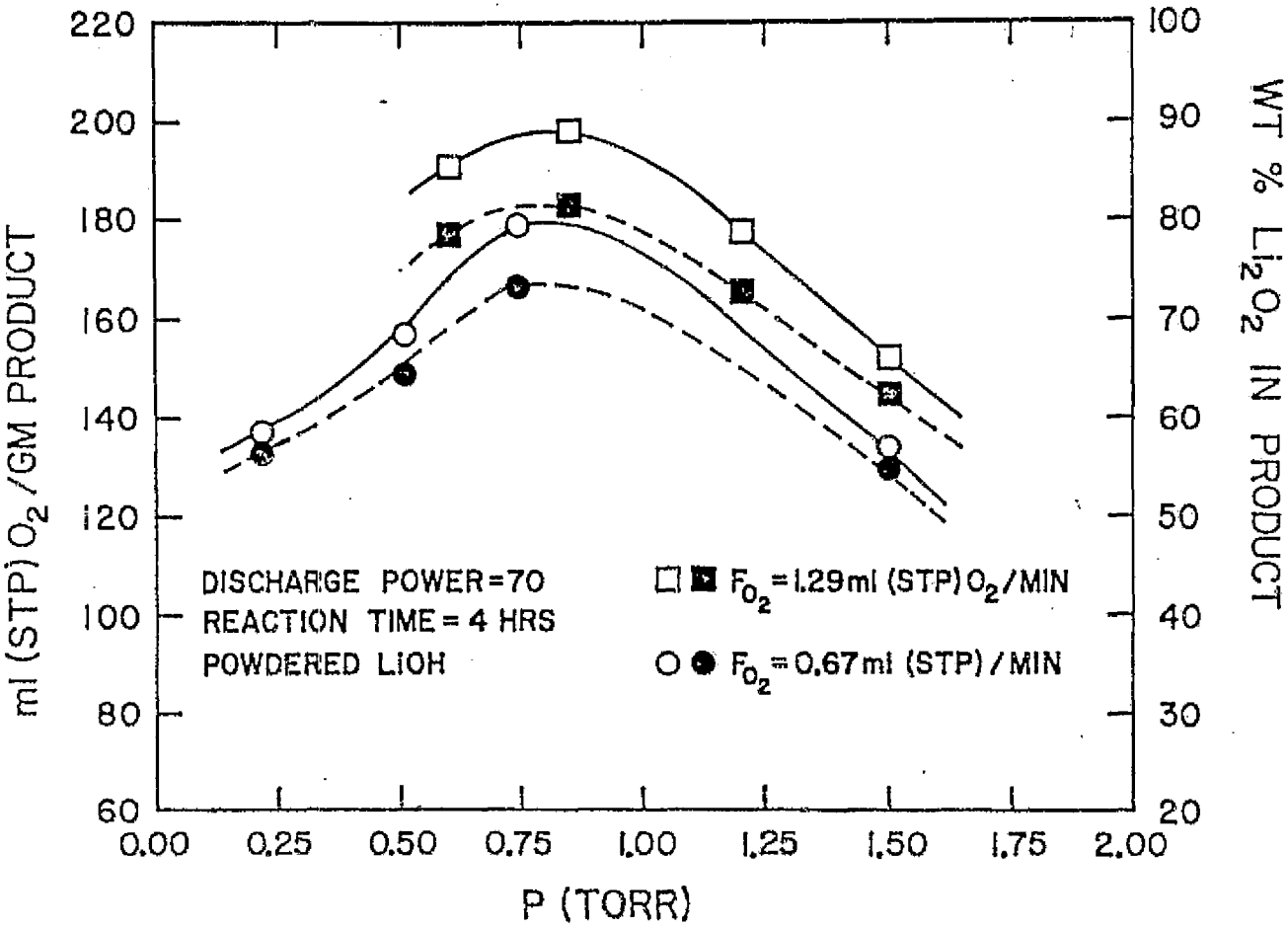

Figure 10. Available O_2 and Weight Percent Li_2O_2 vs. Discharge Pressure for LiOH as the Initial Reactant

lithium. It has been shown by the calculation of standard free energies of formations that although the formation of LiO_2 is thermodynamically feasible the compound is thermodynamically unstable with respect to the lower oxides of lithium by about 15 kcal at room temperature. The formation of LiO_2 by subjecting LiOH to the discharge is also shown to be feasible. However, due to thermodynamic unstability LiO_2, if formed, would decompose to lower oxides unless the decomposition process is retarded by kinetic stability. Furthermore, below 400°K Li_2O_2 is slightly more stable and above 400°K it is slightly less stable than Li_2O. Hence the formation of Li_2O_2 can be anticipated under discharge conditions.

The discharge pressure is found to have a similar effect, as in case of KOH, on the extent of conversion of LiOH to Li_2O_2 - the conversion passing through a maximum with increasing pressure. The maximum conversion for both the flow rates considered takes place at about 0.7 to 0.8 torr. This is approximately the same range of pressure for which the maximum conversion for KOH is found to occur. The flow rate of O_2 also has a very significant effect on the conversion of LiOH to Li_2O_2. The formation of Li_2O_2 increases with increasing flow rate in contrast to the case of KOH for which conversion decreases with increasing flow rate.

The maximum content of Li_2O_2 corresponds to 82% by weight, which occurs at about 0.80 torr and 1.29 ml (STP)/min.

4.2.3. Experiments With $Ca(OH)_2$

The observations during the experiments with $Ca(OH)_2$ were very similar to those with LiOH. No "melting" or increase of pressure was observed during the reaction. Since no "melting" took place, the final product taken for analysis was from the portion of the boat, which was inside the glow of the discharge. Also, the effect of regrinding of the material on the conversion was not investigated since the $Ca(OH)_2$ was available in the form of very fine particles.

The results of the experiments with $Ca(OH)_2$ are shown in Figs. 11 and 12. In Fig. 11 the amount of O_2 available from the product has been plotted as a function of discharge pressure. Fig. 12 shows the weight percent of CaO_2 which has been calculated from the total O_2 represented in Fig. 11. Thus, no formation of $Ca(O_2)_2$ was observed - all the O_2 coming from CaO_2. As in case of LiO_2, calculations indicate that although the formation of $Ca(O_2)_2$ is thermodynamically feasible the compound is unstable with respect to the lower oxides of calcium by about 60 kcal at room temperature. Hence, either $Ca(O_2)_2$ will not form at all or, if

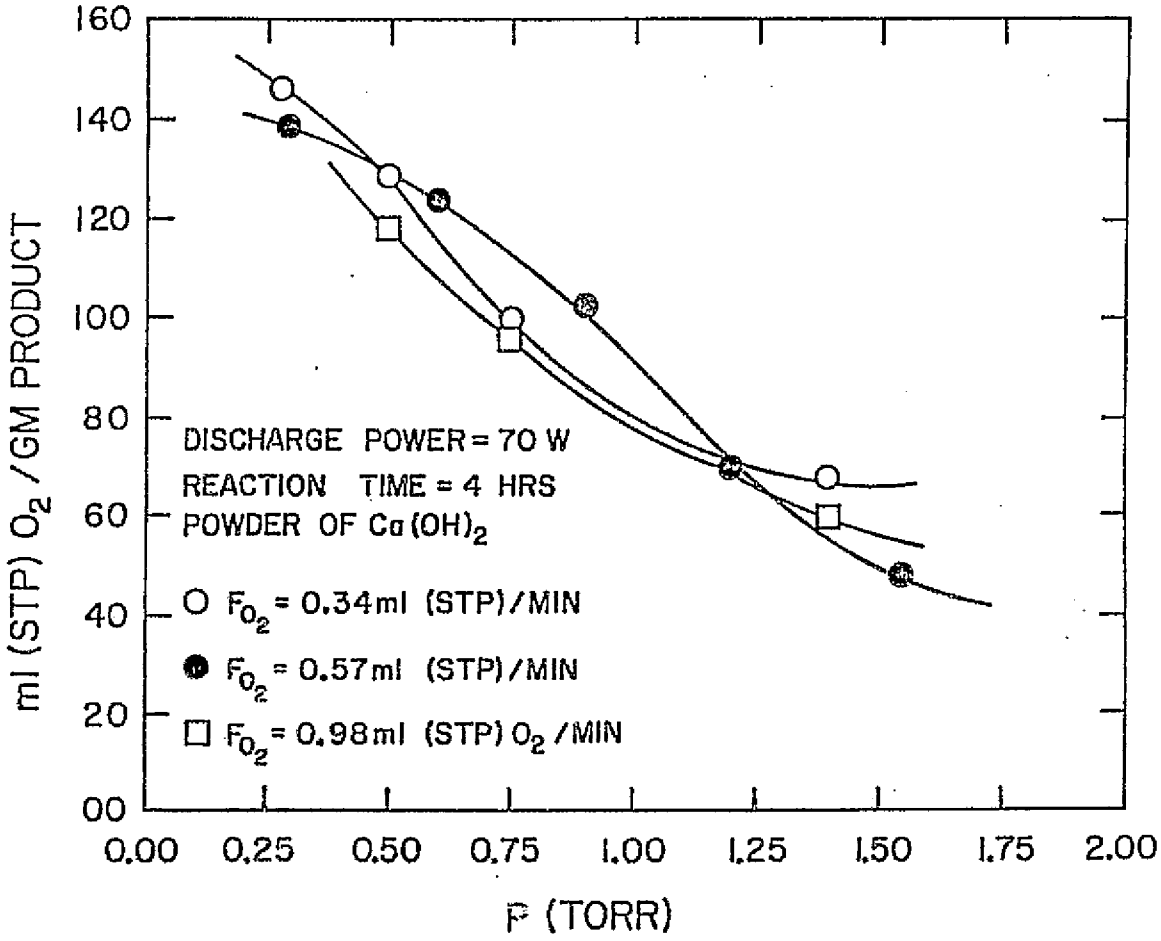

Figure 11. Available O_2 vs. Discharge Pressure for $Ca(OH)_2$ as the Initial Reactant

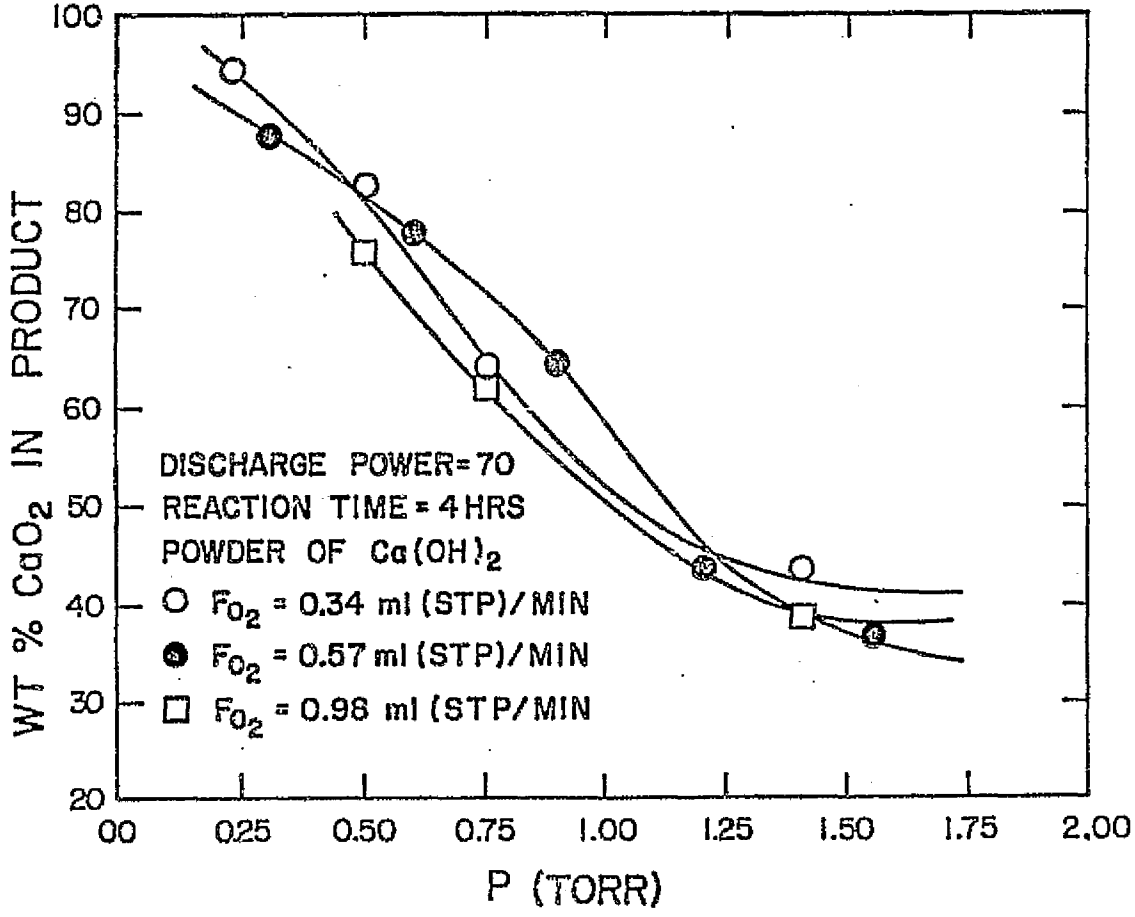

Figure 12. Weight Percent CaO_2 vs. Discharge Pressure for $Ca(OH)_2$ as the Initial Reactant

formed, it will decompose to the lower oxides unless the superoxide is kinetically stable. Furthermore, as has been mentioned in Chapter 2, below 300°K CaO_2 is slightly more stable than CaO and above 300°K it is slightly less stable than CaO. Consequently, CaO_2 is a relatively stable compound. It may thus be concluded that the formation of CaO_2 and the absence of $Ca(O_2)_2$ are not unexpected since these results are consistent with what one might expect from thermodynamics.

It is observed in Figs. 11 and 12 that the effect of discharge pressure on the conversion of $Ca(OH)_2$ to CaO_2 is very pronounced. The conversion falls continually with increasing pressure in contrast to the observations in cases of KOH and LiOH for which the conversion passes through a maximum with increasing pressure. In contrast to observations for experiments with KOH and LiOH the flow rate of O_2 does not seem to have any significant effect on the conversion of $Ca(OH)_2$ to CaO_2. The maximum content of CaO_2 is 88% which is obtained at the lowest experimental pressure of about 0.25 torr.

4.3. KINETICS AND REACTION MECHANISM

An electric discharge sustained in gaseous oxygen produces atomic oxygen and excited state ($a^1\Delta g$, $b^1\Sigma_u^+$) molecular oxygen commonly known as signlet oxygen and represented as O_2^*. These are the two active species present in predominant concentration and both are known to have strong oxidizing capabalities. The rate constant for the dissociation of O_2 to atomic oxygen has been calculated by Bell (34) and is found to be 6.2×10^{-11} cm^3/sec at an average electron energy of 2 eV. Similar calculation for the formation of O_2^* gives the corresponding rate constant to be 2.1×10^{-12} cm^3/sec. at the same average electron energy. Although the rate constants for the formation of O_2^* is an order of magnitude lower than that for atomic oxygen, the life-time of O_2^* particularly that in the $a^1\Delta g$ state is known to be much longer than that for atomic oxygen (35,36). Thus the concentrations of both the species may have comparable magnitude. The typical total concentration of these two species is 20 - 40% of the plasma(34, 35).

It has been indicated by Hollahan and Wydeven (13) from a limited number of experiments that both atomic and excited state molecular oxygen can oxidize

alkali hydroxides to higher oxides. The effect of each of these species on the conversion processes has not been investigated separately. During the formation of superoxides from alkali hydroxides in a discharge it is likely that the formation of peroxides occur in the first step followed by a subsequent conversion of the peroxides to superoxides. Either atomic O or O_2^* could serve as the active species for each of these stages. While Hollahan and Wydeven (13) have suggested a reaction mechanism for the conversion of hydroxide to peroxide and superoxide based only on the atomic oxygen, a plausible reaction mechanism based on the excited state molecular oxygen can also be suggested as shown below.

$$2MOH + O_2^* = M_2O_2 + OH \qquad (4\text{-}1)$$

$$2OH = H_2O + \tfrac{1}{2}O_2 \qquad (4\text{-}2)$$

$$M_2O_2 + O_2^* = 2MO_2 \qquad (4\text{-}3)$$

In support of this mechanism is the observation that KO_2 has been synthesized (37) in 20% yield by oxidizing KOH with O_2 at 1 atm. and 210°C. The yield increases to 34% at 510°C (38). Also according to Kazarnovskii (39) the transition of peroxide to superoxide takes place

via the reaction:

$$M_2 (O - O^{2-}) + O_2 = 2M (O - O^{-}) \qquad (4-4)$$

Thus molecular oxygen can oxidize both KOH and K_2O_2 to KO_2. In view of this, similar reactions should take place with O_2^* and should proceed at a higher rate.

The mechanisms for solid-gas reactions in a discharge environment are probably more complex than those suggested on the basis of either atomic oxygen or excited state moledular oxygen. As evidence for this we can compare the present observations with those of Vol'nov and co-workers (12). In their work a dc discharge was used to obtain higher oxides of alkali and alkaline earth metals. The yield of KO_2 was 80% by weight. Use of $Ca(OH)_2$ produced 4% of CaO_2 in 30 minutes, whereas LiOH did not produce any Li_2O_2 at all. In these experiments the material was placed in the positive column of the dc discharge. For such an arrangement the concentrations of the active species are known to vary with the position in the discharge tube. Thus, experiments for synthesis of NH_3 in dc discharge indicate that the rate of formation of NH_3 in the negative column is much greater than in the positive column (40).

If atomic oxygen is taken to be responsible for the reactions, then the effect of pressure on the conversion can be explained. It has been shown by Bell and Kwong (41) that for a RF discharge in oxygen the concentration of atomic oxygen increases with pressure, passes through a maximum and then decreases slowly with further increase of pressure. In the case of the experiments with KOH and LiOH the variation of the conversion to higher oxides behave in a manner similar to that of atomic oxygen concentration. It is further observed that the maxima for the higher oxides from both the hydroxides and for the concentration of atomic oxygen occur in the same range of pressure, namely 0.6 - 1.1 torr. However, in case of experiments with $Ca(OH)_2$ no maximum for CaO_2 was observed, the conversion falling continually from the starting pressure of 0.25 torr. While it is possible, that a maximum might occur at a pressure below 0.25 torr, this seems unlikely.

The effect of flowrate on the conversion of KOH to higher oxides can be interpreted in terms of the effects of flow rate on the concentration of atomic oxygen. Bell and Kwong (41) have shown that concentration of atomic oxygen decreases with increasing flow rate of O_2 due to reduction of the residence time in the

discharge. This trend could explain the lower conversion to higher oxides of potassium with increased flow rate of O_2. However, in case of LiOH the conversion increases with increasing flow rate and this effect is difficult to explain simply from the consideration of atomic oxygen. The conversion in case of experiments with $Ca(OH)_2$ appears to be independent of the flow rate of O_2.

As seen in Fig. 9 the conversion of KOH to the higher oxides increases with increasing discharge power, passes through a maximum and then decreases with further increase of power. This observation could be interpreted as follows. Bell and Kwong (41) has shown that the concentration of atomic oxygen increases with increasing discharge power. Thus, if atomic oxygen is responsible for the formation of the higher oxides then the conversion should increase continually. However, with increasing power the spread of the "melting" of potassium hydroxide also increases and at relatively high discharge power almost all the material in the boat appears to "melt". As mentioned previously, the melting causes the formation of a thin crust which is not favorable for high conversion. The "melting" and the subsequent formation of the crust are believed to more than offset the effect of increase of concentration

of atomic oxygen with discharge power. As a result the conversion of KOH to the higher oxides will tend to decrease with increasing power.

The rapid "melting" of the potassium hydroxide observed during the experiments is also believed to be associated with the interaction of atomic oxygen and other activated species with the potassium hydroxide on the boat. The potassium hydroxide used in the present work contained about 5% water which forms a double compound having the general formula $KOH \cdot xH_2O$. The energy evolved due to the recombination of the atomic oxygen and the deactivation of other active species on the surface of the solid hydroxide is utilised to decompose the double compound. The water released by this process dissolves KOH and the solution of KOH appears as a "molten" material on the boat. Although water is formed during the conversion of the KOH to the higher oxides as shown in eqn. (4-2), the rate of formation of water is likely to be slow. In view of this it appears that the water formed during the reaction (4-2) does not contribute to the "melting" process which was observed to be very rapid.

Although the gas temperature in the discharge has not been measured in the present work, application of the correlation developed by Brown and Bell (42)

has shown that the gas temperature is about 90-100°C, which is much lower than the melting point (360°C) of KOH. Hence, actual melting of KOH does not occur, instead the water released from the double compound dissolves the KOH as explained in the preceding paragraph.

Although some of the effects of reaction conditions on conversion of metal hydroxides to higher oxides have been explained by considering the variation of atomic oxygen concentration with the discharge parameters, it is believed that the effects of both atomic oxygen and excited state molecular oxygen must be taken into account. Elucidation of the role of each of these epecies in the reactions and the measurement of the concentrations of the excited state molecular oxygen in addition to that of atomic oxygen might explain more convincingly the changes in the conversion with changes in the operating variables.

4.4. RESULTS AND DISCUSSION OF THE THERMAL ANALYSIS OF A MIXTURE OF HIGHER OXIDES OF POTASSIUM

4.4.I. Thermogravimetric Analysis

The thermogravimetric analyses (TGA) of the commercial samples of KO_2 and the product obtained by subjecting KOH to discharged oxygen are shown in Figs. 13 and 14. As seen from the figures, two thermogravimetric analyses, TGA 1 and 2 of the same batch of the commercial sample were performed. Two additional analyses, TGA 3 and 4, of the materials produced at 50 and 70 watts of discharge power were also performed. As mentioned previously, the first analysis, TGA 1, was conducted up to 700°C, while the remaining thermograms shown for TGA 2,3, and 4 in Figs. 13 and 14 have only been illustrated up to 775-850°C. This was done because it was observed that from about 700°C upwards the weight loss occured continuously without any additional features characteristic of the onset of a new process until 90% or more of the material had been lost at 1100°C.

It is observed from Figs. 13 and 14 that except for minor deviation in TGA 4 the weight loss of the materials as a function of temperature follows the

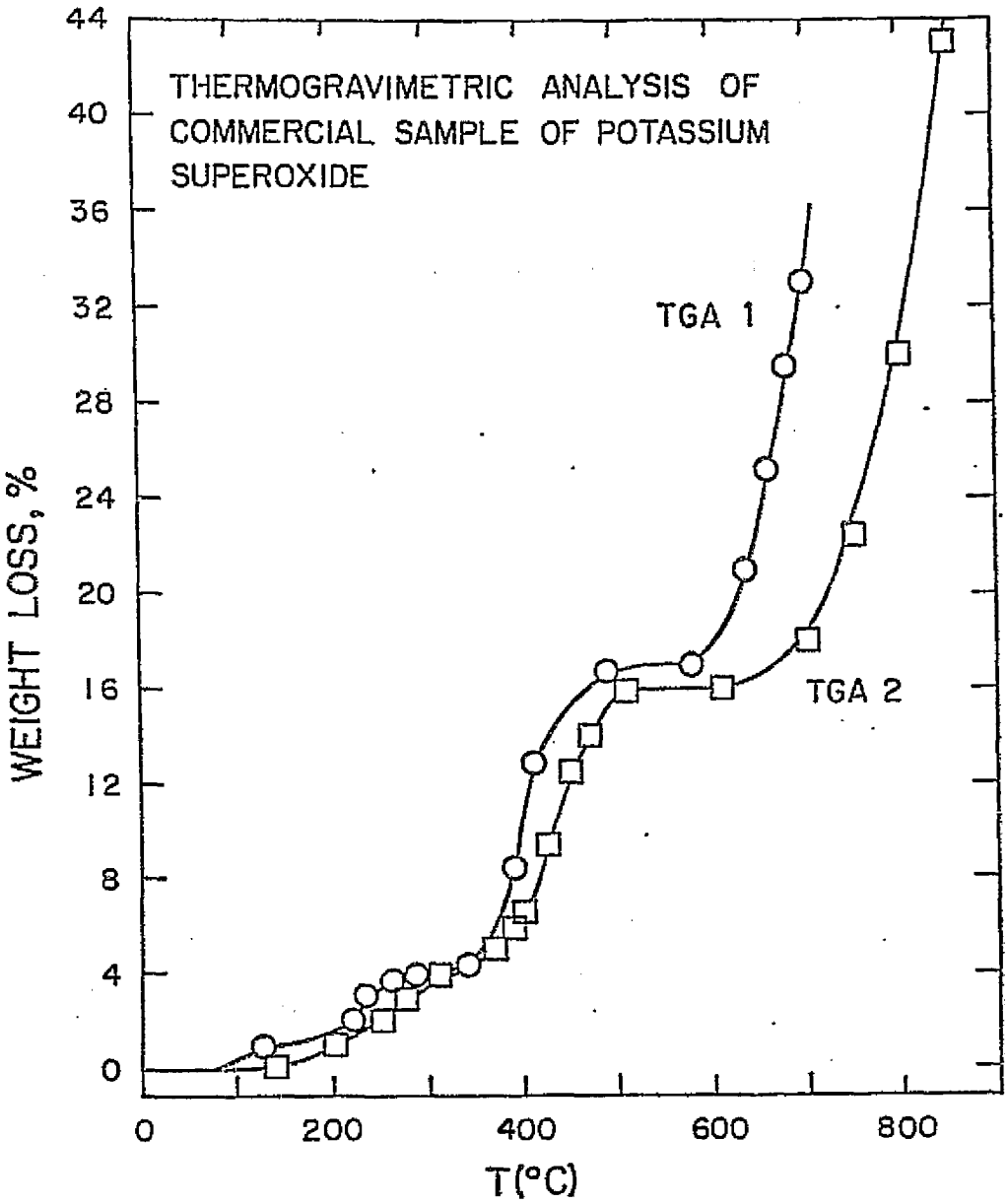

Figure 13. Thermogravimetric Analysis of Commercial Sample of Potassium Superoxide

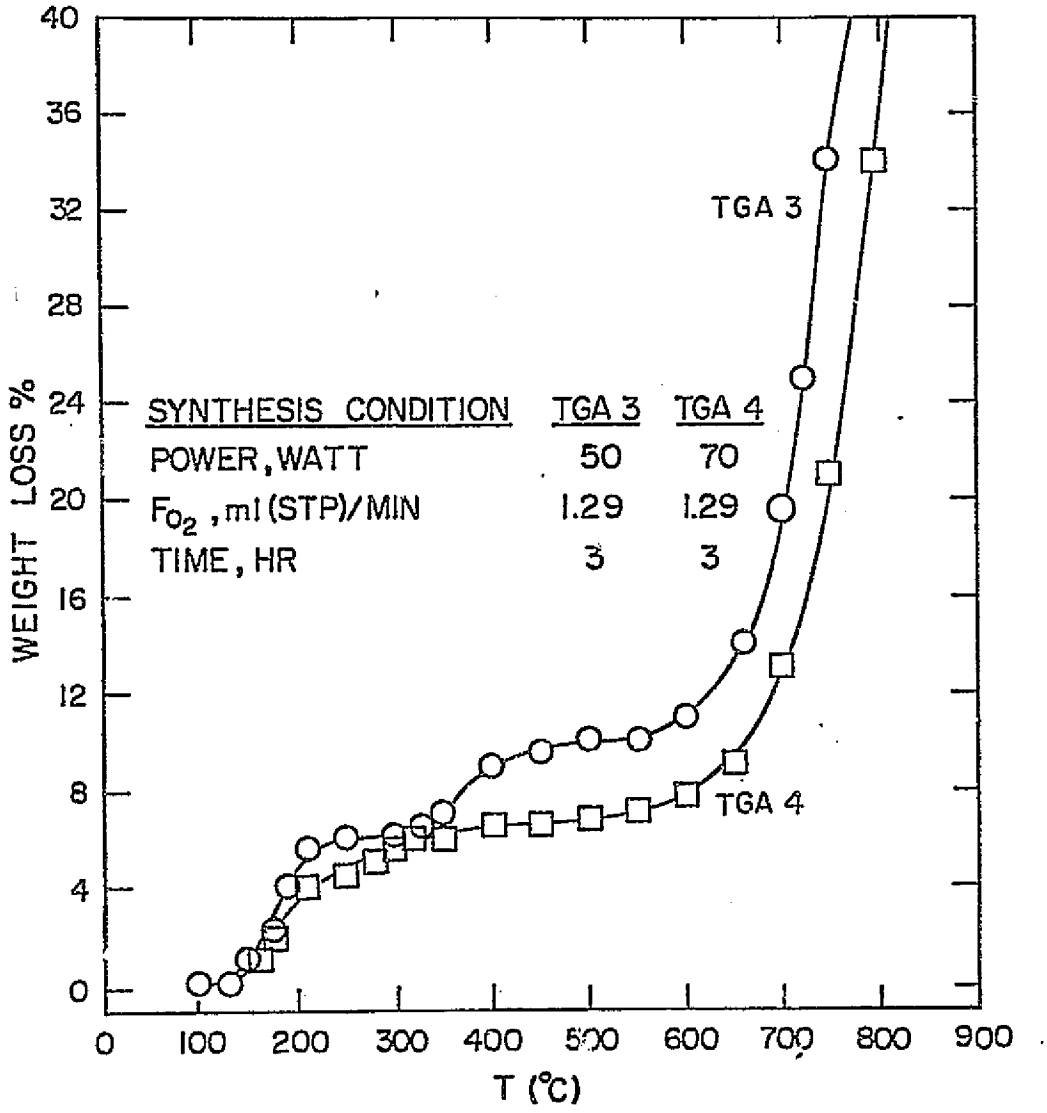

Figure 14. Thermogravimetric Analysis of the Mixture of Higher Oxides of Potassium Prepared by the Discharge Method

same pattern in all cases. Thus, for TGA 1, 2, and 3 the significant weight loss takes place in three temperature ranges, 125 to 250°C, 350 to 500°C, and 600 to 1100°C. The weight loss in the first and second temperature range is followed by the occurence of a plateau during which little or no weight loss takes place. For TGA 4 the first plateau is not as prominent as in the remaining three. Similarly, the weight loss in the second temperature range for this analysis is not quite as sharp. It is further observed that up to about 325°C, the weight loss for the commercial sample in TGA 1 and 2 is about 6% whereas for the samples prepared by the discharge method the corresponding weight loss is about 4%.

Fig. 13 indicates that except for the end of the first plateau the weight loss for TGA 1 is always higher than that for TGA 2. This effect is more pronounced for temperatures above 600°C. If the weight loss is limited by the diffusion of gaseous oxygen from the boundary of the samples then the above difference can be attributed to the difference in flowrate of the inert gases during the two analyses. The flow rate during TGA 1 was 2-3 cu.ft./hr. whereas for TGA 2 only 0.7 cu.ft./hr. Higher flow rate would enhance the transport of O_2 from the surface of the material.

It is apparent from Fig. 14 that the thermograms for the two samples prepared by the discharge technique are not identical. In this instance, however, the flow rate of the inert gas is the same and hence the differences must be ascribed to the differences in the composition of the samples, As we shall see later the two samples contain different amounts of KO_2.

The weight loss in the different temperature ranges and the occurence of the plateaus can be explained as follows. The weight loss for all four analyses, TGA 1 to 4, starts at about 125°C. It is believed that this weight loss is due to the decomposition of KO_2 by the reaction.

$$2KO_2\ (s) = K_2O_2\ (s) + O_2\ (g) \qquad (4\text{-}5)$$

This view is supported by the observation of Rode (43) who reported that decomposition of KO_2 starts at 145°C. Although the temperature at which the decomposition of KO_2 is observed to start in the present work is somewhat lower than Rode's value, differences of similar magnitude are not uncommon in thermal analyses. In any event, the decomposition continues up to about 250°C after which the first plateau begins its appearance.

During the occurence of the first plateau between about 250 to 350°C little or no decomposition takes place. One possible explanation for this is that K_2O_2 formed below 250°C as well as any K_2O_2 present in the original sample forms a solid solution with the remaining KO_2 and hence makes the material thermally stable. Such a stabilization would retard the weight loss until a much higher temperature was reached to decompose the solid solution and hence the KO_2. The formation of a solid solution between KO_2 and K_2O_2 has been indicated by Vol'nov (1). Furthermore, the formation of a solid solution between analogous compounds such as NaO_2 and Na_2O_2 at about 260°C has been reported by Marriott, Capotosto and Petrocelli(44).

Over the temperature range of the first plateau there is also the possibility of formation of a solid solution involving KOH in addition to KO_2 and K_2O_2. This possibility is suggested from analogy of the formation of a solid solution involving NaO_2, Na_2O_2 and NaOH as indicated by Volnov (1). The presence of KOH in the samples analysed in the present work could easily be justified. For example, a small quantity of the unreacted KOH is likely to be present in the product synthesized in the discharge. In case of the commercial sample which is prepared from metallic potassium

the presence of a trace quantity of water could explain the occurence of KOH.

After the first plateau further weight loss occurs at about 325-350°C, indicating the decomposition of the solid solution and hence the decomposition of the residual KO_2 released from the solid solution. This decomposition continues up to about 475-500°C according to the reaction indicated previously. For the commercial sample the weight loss in this temperature range is more than in the first temperature range mentioned before.

At the end of the second temperature range the second plateau begins to appear. The plateau extends from about 475°C to 600°C. In this temperature range no weight loss has been observed for any of the thermogravimetric analyses. Over this temperature range K_2O_2 which melts at 490°C (45) is thermally stable. Calculations show that decomposition pressures of K_2O_2 are 0.08 and 0.29 torr at 565°C and 627°C respectively. Thus, it is obvious that no significant weight loss should be observed until about 600°C, a conclusion validated by the observations of all four analyses.

Above 600°C K_2O_2 decomposes rapidly according to the reaction

$$K_2O_2\ (l) = K_2O\ (s) + \tfrac{1}{2}O_2 \qquad (4\text{-}6)$$

The weight loss is rapid in this temperature range. At still higher temperatures K_2O starts decomposing, the decomposition pressure being 600 torr at 881°C.

Since the weight loss up to 600°C is due to the decomposition of KO_2 according to the reaction

$$2KO_2 = K_2O_2 + O_2 \qquad (4\text{-}7)$$

This quantity can be used to determine the amount of KO_2 present in the samples. The same samples have been analyzed by the method of Seyb and Kleinberg as described previously. However, the amount of KO_2 determined on the basis of O_2 evolved in the first step of analysis is not reliable because of the reason stated before. Nevertheless, valuable information would be generated by comparing the equivalent weight percent KO_2 calculated from the total oxygen evolved in that method with the absolute weight percent KO_2 calculated from the TGA results.

Table 8 shows that the absolute amount of KO_2 determined by the thermal analyses is consistently lower than the equivalent weight perecnt of KO_2 determined by the wet chemical method of Seyb and

Table 8

Comparison Of Results Of Analyses Of Mixture Of Higher Oxides Of Potassium By Thermal And Wet Chemical Method

Sample	Equivalent Weight Percent KO_2 By Wet Chemical Method	Weight Percent KO_2 By TGA
Commercial (TGA 1)	82.0	75.5
Commercial (TGA 2)		71.0
Prepared (TGA 3)	60.9	44.4
Prepared (TGA 4)	69.3	31.0

Kleinberg (32). Since the equivalent weight percent of KO_2 has been calculated from the total oxygen released from KO_2 as well as K_2O_2 the absolute weight percent of KO_2 must be lower than the former quantity. The results of the thermal analyses are in comformity with this behavior. Furthermore, although the percent purity of the commercial sample with respcet to K_2O_2 was not known this quantity is never more than a few percent (46). Hence, the weight percent of KO_2 in the commercial sample would be less than but close to 82%. Both the thermal analyses of the commercial sample are consistent with this expectation. And these observations lead to the conclusion that the thermogravimetric technique is a superior method for determining the amount of KO_2 in a mixture of higher oxides of potassium.

Before the conclusion of the discussion of the TGA results, attention may be drawn to the fact that thermal behavior of KO_2 has been reported by a number of workers but without any agreement concerning the results. Thus Blumenthal (47) reports the melting point, presumably without decomposition, of KO_2 to be 380°C. The corresponding value reported by de Forcrand (48) is 440°C. Considering the persistent beginning of decomposition at about 125°C in all the analyses in

the present work and the comparable value of 145°C reported by Rode (43) the values reported by Blumenthal and de Forcrand are difficult to justify.

4.4.2. Differential Thermal Analysis

To gain insight into the thermal behavior of the oxides of potassium and to verify the occurence of various thermal changes during the thermogravimetric analyses complementary differential thermal analyses were performed. One DTA each of the commercial sample and the sample prepared at 70W is presented in Fig. 15.

It is observed from Fig. 15 that up to about 225°C the DTA for both samples show very similar features. However, beyond 225°C the DTA for the commercial sample shows more pronounced features. Nevertheless, the curve for the sample prepared by the discharge method is qualitatively similar to that for the commercial sample.

Fig. 15 shows two exothermic peaks in the first temperature range (125 - 250°C), over which significant weight loss of the materials takes place (see Figs. 13 and 14). The first of these two peaks is believed to be associated with the decomposition of KO_2 as well as phase transformation of KO_2, which occurs from the

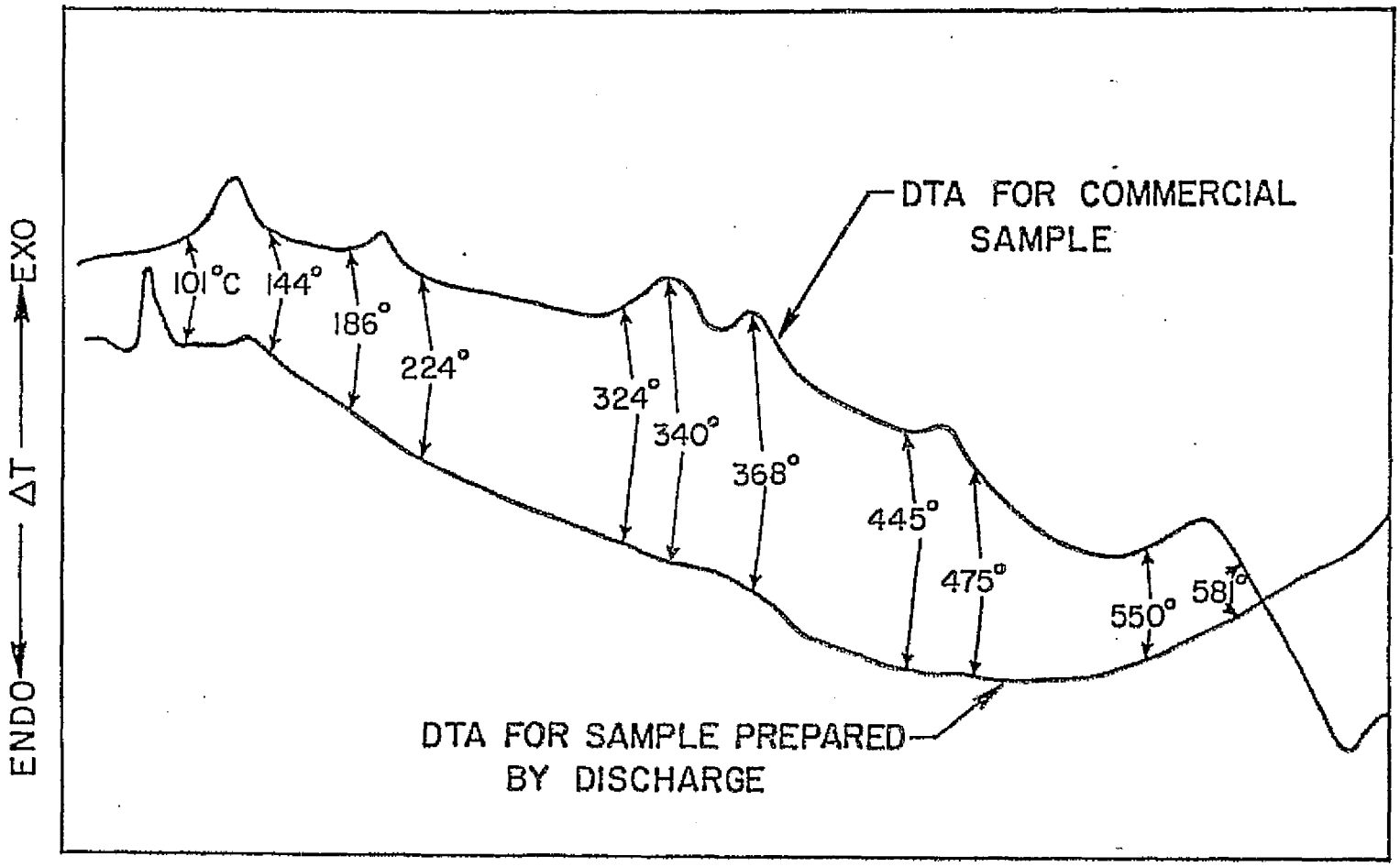

Figure 15. Differential Thermal Analysis of the Commercial Sample of Potassium Superoxide and the Mixture of Higher Oxides of Potassium Prepared by the Discharge Method

α to the β form. The α-KO_2 is stable between -75 and 100°C, whereas above 100°C α-KO_2 transforms to the β form. The second peak is associated only with KO_2 decomposition.

During the discussion of the TGA results it was mentioned that formation of a solid solution takes place over the temperature range of the first plateau (250 - 350°C). Since the formation of a solid solution is an exothermic process this view is supported by the appearance of a very pronounced exotherm at about 324°C. In addition to this exotherm a second exotherm also seems to appear at about 356°C. This could conceivably result from the heat effect associated with the formation of a solid solution. As in the discussion of TGA results an analogy can be drawn from the corresponding behavior of the oxides of sodium. Thus, formation of an exotherm in the vicinity of 260°C where solid solution formation occurs has been observed by Marriot, Capotosto and Petrocelli (44) during the study of the thermal behavior of NaO_2.

It is further observed that above 368°C both the DTA curves indicate, in general, that a very strong endothermic process is taking place. This could be attributed to the sharp decomposition of the superoxide which starts after the occurence of the first plateau observed in the TGA results.

CHAPTER 5

CONCLUSION

Potassium hydroxide when subjected to electrically discharged oxygen produces both potassium peroxide and potassium superoxide. The extent of conversion to the higher oxide strongly depends upon the particle size of the KOH, the relative position of KOH in the discharge zone and the operating conditions of the discharge i.e. the power, pressure, and flow rate of oxygen. The maximum conversion of KOH expressed in terms of the equivalent weight percent of KO_2 is 75% which occurs at a pressure of 0.95 torr, a discharge power of 70 watts, and an oxygen flow rate of 1.29 ml(STP)/min. The reaction time for maximum conversion is 3 hrs.

Hydroxides of lithium and calcium do not form superoxides in the presence of an oxygen discharge but instead are converted to peroxides. The percentage of Li_2O_2 and CaO_2 in the products strongly depends upon the operating variables of the discharge. In the case of experiments with LiOH the maximum content of Li_2O_2 in the product is 82% by weight, which occurs at 0.9 torr, a discharge power of 70 watts, and an oxygen flowrate of 1.29 ml(STP)/min. The reaction time for

this conversion is 4 hrs. For the experiments with $Ca(OH)_2$ the maximum extent of CaO_2 is about 94% by weight, which occurs at 0.25 torr the lowest experimental pressure) and a flow rate of 0.34 ml(STP)/min. The reaction time and the discharge power are the same as for the maximum yield of Li_2O_2.

The absence of LiO_2 and the formation of Li_2O_2 can be explained from the thermodynamic properties of the oxides of lithium. Lithium superoxide is known to to be thermodynamically unstable with respect to the lower oxides. Below 400°K Li_2O_2 is more stable than Li_2O, while above 400°K Li_2O is more stable than Li_2O_2. Thus one must conclude that if LiO_2 is formed then it rapidly decomposes to Li_2O_2 unless the temperature is significantly above 400°K. Alternatively, it is also possible that Li_2O_2 is formed directly but does not undergo further oxidation to LiO_2.

To explain the absence of $Ca(O_2)_2$ in the corresponding product obtained from $Ca(OH)_2$ the standard free energy of formation of $Ca(O_2)_2$ was determined theoretically. For this purpose the enthalpy of formation was evaluated using a Born-Haber cycle. As a part of this computation the lattice energy of $Ca(O_2)_2$ was calculated using the Born-Mayer method.

The other important quantities involved in the Born-Haber cycle were taken from the literature. The standard entropy change was determined using the latimer's ion contribution technique.

From these calculations it was concluded that $Ca(O_2)_2$ is highly unstable with respect to the lower oxides of calcium. Below 300°K CaO_2 is slightly more stable than CaO and above 300°K slightly less stable than CaO. These observations suggest that $Ca(O_2)_2$, if formed, is likely to decompose to the lower oxides. If the temperature is not significantly above 300°K $Ca(O_2)_2$ would decompose to CaO_2. The absence of any $Ca(O_2)_2$ from the experimental results led to the conclusion that either $Ca(O_2)_2$ does not form at all or that its decomposition is very rapid. In the event that $Ca(O_2)_2$ does not form at all the formation of CaO_2 takes place directly from $Ca(OH)_2$.

While it has not been possible to define a mechanism for the synthesis of the products found in this work, the dependence of the yields of KO_2 upon oxygen pressure and flow rate can be explained. The observation of a maximum in product yield near 1 torr and the decline in yield with increased flow rate support the conclusion

that atomic oxygen is the primary discharge product involved in the oxidation of the starting hydroxide. This conclusion is based on the observation that a maximum in the concentration of atomic oxygen is known to occur near 1 torr and the fact that an increase in flow rate produce a reduction in the concentration of atomic oxygen. The behavior of $Ca(OH)_2$ is substantially different form that of KOH or LiOH. In this instance the only product formed is CaO_2. The yield of this product declines with increasing pressure but does not pass through a maximum over the pressure range studied. No definite effect of flow rate could be observed on yield of CaO_2. These differences in the effects of pressure and flow rate can not be explained at present and may be associated in part with differences in the chemistry which alkali and alkaline earth metal hydroxides undergo in a discharge.

Finally it was noted in the course of the present work that the analytical method developed by Seyb and Kleinberg for the determination of the amount of superoxide present in product could give inaccurate results if both peroxide and superoxide anions were present in the product. Thus while the method does give an accurate measure of the total amount of oxygen which can be released from the product, the superoxide content

is usually over estimated. An alternative method based upon thermogravimetric analysis was investigated for the case of the products produced from KOH. Interpretation of the TGA results showed that the total weight loss occurring between 125°C and 500°C could be associated with KO_2 alone, since K_2O_2 does not decompose below 500°C.

The fact that KO_2 can be synthesized in an oxygen discharge is encouraging and should be investigated further in order to determine whether this product can be made in high purity. The present process for KO_2 manufacture uses molten potassium metal which is atomized into a chamber filled with oxygen at 1.2 atm and 300°C. The principal disadvantage of this system is the requirement of metallic potassium which is expensive and difficult to handle. The present approach which starts with the hydroxide, which is cheaper than the metal, could offer a possible alternative if the product could be obtained in good yield and with only modest consumption of electricity.

The use of a discharge to synthesize Li_2O_2 and CaO_2 may also have some attraction. Both of these materials are presently made by reacting the metal hydroxide with H_2O_2. Particularly in the synthesis of Li_2O_2, the H_2O_2 must be used in high concentration and the product must be

dried using an elaborate arrangement. By contrast the discharge approach appears to be capable of providing the product in dry form by a one step process.

APPENDIX - A

EXPERIMENTAL DATA

The data obtained in the experiments with KOH are given in Tables A - 1 to A - 4. The results calculated from these data are represented in Figs. 8 and 9 and in Table 7. The data from the experiments with LiOH and $Ca(OH)_2$ are shown in Tables A - 5 to A - 9 and the corresponding results are represented in Figs. 10 to 12.

Table A - 1

Experiment With KOH

Serial No.	Particle Size	Flowrate Of O_2 (ml(STP)/min)	Pressure (torr)	Power (watt)	Reaction Time (hr)	Mass Of Product Taken For Analysis (mg)	STP Volume Of O_2 Released At first Step Of Analysis (ml)	STP Volume Of O_2 Released At Second Step Of Analysis (ml)
1.	Coarse Grit	2.78	0.95	70	3	187.0	2.08	2.06
2	Powder	2.78	0.95	70	3	72.7	2.26	2.54
3.	Powder	2.78	0.95	70	3	72.9	2.55	1.58

Table A - 2

Experiment With KOH

Serial No.	Particle Size	Flowrate Of O_2 (ml(STP)/min)	Pressure (torr)	Power (watts)	Reaction Time (hr)	Mass Of Product Taken For Analysis (mg)	STp Volume Of O_2 Released At First Step Of Analysis (ml)	STP Volume Of O_2 Released At Second Step Of Analysis (ml)
1.	Fine Powder	1.29	0.54	70	6	37.9	2.06	1.03
2.	Fine Powder	1.29	0.73	70	6	48.3	4.04	1.88
3.	Fine Powder	1.29	0.95	70	6	38.9	3.70	1.88
4.	Fine Powder	1.29	1.24	70	6	30.5	2.13	1.04

Table A - 3

Experiment With KOH

Serial No.	Particle Size	Flowrate Of O_2 (ml(STP)/min)	Pressure (Torr)	Power (Watts)	Reaction Time (hr)	Mass Of Product Taken For Analysis (mg)	STP Volume Of O_2 Released At First Step Of Analysis (ml)	STP Volume Of O_2 Released At Second Step Of Analysis (ml)
1.	Fine Powder	0.67	0.30	70	6	18.1	1.63	0.53
2.	Fine Powder	0.67	0.60	70	6	21.7	2.53	0.71
3.	Fine Powder	0.67	1.10	70	6	35.1	1.06	4.21
4.	Fine Powder	0.67	1.45	70	6	27.7	1.79	2.04

Table A - 4

Experiment With KOH

Serial No.	Particle Size	Flowrate Of O_2 (ml(STP)/min)	Pressure (torr)	Power (watt)	Reaction Time (hr)	Mass Of Product Taken For Analysis (mg)	STP Volume Of O_2 Released At First Step Of Analysis (ml)	STP Volume Of O_2 Released At Second Step Of Analysis (ml)
1.	Fine Powder	1.29	0.95	50	3	16.0	1.68	0.62
2.	Fine Powder	1.29	0.95	70	3	10.9	1.19	0.76
3.	Fine Powder	1.29	0.95	90	3	20.8	2.35	0.71

Table A - 5

Experiment With LiOH

Serial No.	Particle Size	Flowrate Of O_2 (ml(STP)/min)	Pressure (orr)	Power (att	Reaction Time (hr)	Mass Of Product Taken For Analysis (mg)	STP Volume Of O_2 Released At Second Step Of Analysis (ml)
1.	Fine Powder	0.67	0.21	70	4	14.0	1.92
2.	Fine Powder	0.67	0.51	70	4	12.5	1.96
3.	Fine Powder	0.67	0.74	70	4	9.7	1.73
4.	Fine Powder	0.67	0.96	70	4	9.9	1.32
5.	Fine Powder	0.67	1.50	70	4	10.5	1.42

Table A - 6

Experiment With LiOH

Serial No.	Particle Size	Flowrate Of O_2 (ml(STP)/min)	Pressure (torr)	Power (watt)	Reaction Time (hr)	Mass Of Product Taken For Analysis (mg)	STP Volume Of O_2 Released At Second Step Of Analysis (ml)
1.	Fine Powder	1.29	0.60	70	4	13.2	2.51
2.	Fine Powder	1.29	0.85	70	4	15.3	3.03
3.	Fine Powder	1.29	1.20	70	4	15.2	2.70
4.	Fine Powder	1.29	1.50	70	4	9.8	1.50

Table A - 7

Experiment With $Ca(OH)_2$

Serial No.	Particle Size	Flowrate Of O_2 (ml(STP)/min)	Pressure (torr)	Power (watt.)	Reaction Time (hr)	Mass Of Product Taken For Analysis (mg)	STP Volume Of O_2 Released At Second Step Of Analysis (ml)
1.	Fine Powder	0.57	0.30	70	4	8.8	1.22
2.	Fine Powder	0.57	0.60	70	4	8.3	1.02
3.	Fine Powder	0.57	0.90	70	4	8.2	0.84
4.	Fine Powder	0.57	1.20	70	4	8.5	0.59
5.	Fine Powder	0.57	1.55	70	4	8.7	0.50

Table A - 8

Experiment With $Ca(OH)_2$

Serial No.	Particle Size	Flowrate Of O_2 (ml(STP)/min)	Pressure (Torr)	Power (Watts)	Reaction Time (hr)	Mass Of Product Taken For Analysis (mg)	STP Volume Of O_2 Released At Second Step Of Analysis (ml)
1.	Fine Powder	0.34	0.23	70	4	7.9	1.16
2.	Fine Powder	0.34	0.50	70	4	7.7	0.99
3.	Fine Powder	0.34	0.75	70	4	8.9	0.89
4.	Fine Powder	0.34	0.40	70	4	8.6	0.58

Table A - 9

Experiment With $Ca(OH)_2$

Serial No.	Particle Size	Flowrate Of O_2 (ml(STP)/min)	Pressure (Torr)	Power (Watts)	Reaction Time (hr)	Mass Of Product Taken For Analysis (mg)	STP Volume Of O_2 Released At Second Step Of Analysis (ml)
1.	Fine Powder	0.98	0.50	70	4	8.80	1.04
2.	Fine Powder	0.98	0.75	70	4	10.06	1.03
3.	Fine Powder	0.98	1.40	70	4	8.90	0.53

APPENDIX - B

SAMPLE CALCULATIONS

The sequence of calculations used to determine the amounts of superoxide and peroxide in the products obtained from experiments with KOH, LiOH and $Ca(OH)_2$ are described below. In case of the analyses with the products from experiments with LiOH and $Ca(OH)_2$ the volume changes of the gas inside the apparatus after adding diethyl phthalate and acetic acid diethyl phthalate mixture are always negligible and hence they were not taken into account.

(1) Sample calculation for the determination of the amount of superoxide and peroxide in the product obtained from experiments with KOH.

Discharge Pressure = 0.92 torr

Flow rate of O_2 = 1.29 ml(STP)/min

Discharge power = 70 watts

Reaction time = 6 hrs (2 steps)

Mass of product taken for analysis = 38.9 mg

Gas buret reading at the ambient temperature ($27^{o}C$) after attaching the reactor and adjustment of the inside pressure to 1 atm

= 1.120 ml

Volume of the inside of the apparatus up to the zero-mark of the buret = 38.43 ml

Total gas volume at 1 atm after attaching the reactor = 38.43 + 1.12 = 39.55 ml at $27.0^{o}C$

Volume of diethyl phthalate added = 1.40 ml

Volume of acetic acid diethyl phthalate solution added = 1.95 ml

The buret reading at the ambient temperature ($25^{o}C$) after completion of the first step of decomposition and adjustment of the inside pressure to 1 atm = 8.20 ml

Gas volume after first step decomposition

= (38.43 + 8.20) - (1.40 + 1.95)

= 46.55 - 3.35

= 43.20 ml at $25^{o}C$

= 43.54 ml at $27^{o}C$

Volume of O_2 evolved at the first step

= 43.54 - 39.55

= 3.99 ml at $27^{o}C$

= 3.63 ml at STP

Weight percent of KO_2 in the sample analyzed:

$$\frac{142 \times 3.63 \times 100}{22.4 \times 10^3 \times 0.0389}$$

$$= 59.24\%$$

Volume of $FeCl_3$ solution added = 2.00 ml

Gas buret reading at the ambient temperature (26^oC) after completion of the second step of decomposition and adjustment of the inside pressure to 1 atm = 12.47 ml

Gas volume after the second step of decomposition

$$= (38.43 + 12.47) - (3.35 + 2.00)$$

$$= 50.90 - 5.35$$

$$= 45.55 \text{ ml at } 26^oC$$

$$= 45.68 \text{ ml at } 27^oC$$

Volume of O_2 evolved at the second step

$$= 45.68 - 43.54 = 2.14 \text{ ml at } 27^oC$$

$$= 1.95 \text{ ml at STP}$$

Total O_2 evolved . . .

$$= (3.63 + 1.95)/0.0389$$

$$= 143.31 \text{ ml (STP)/gm}$$

Equivalent weight percent of KO_2 in the sample analyzed $= \frac{142 \times 143.31 \times 100}{22.4 \times 10^3 \times 1.5}$

$$= 59.68\%$$

(2) Sample calculation for the determination of the amount of peroxide in the product obtained from experiments with LiOH.

Discharge pressure = 0.85 torr

Flowrate of O_2 = 1.29 ml(STP)/min

Discharge power = 70 watts

Reaction time = 4 hrs.

Mass of product taken for analysis = 15.3 mg

Gas buret reading at the ambient temperature (24.1°C) after attaching the reactor and adjustment of the inside pressure to 1 atm = 0.75 ml

Volume of the inside of the apparatus up to the zero-mark of the buret = 38.43 ml

Total gas volume at 1 atm after attaching the reactor = 38.43 + 0.75

= 39.18 ml at 24.1°C

Volume of diethyl phthalate added

= 1.55 ml

Volume of acetic acid-diethyl phthalate mixture added = 1.50 ml

Volume of $FeCl_3$ solution added

= 2.80 ml

Gas Buret reading at the ambient temperature ($22.0^{o}C$) after evolution of O_2 and adjustment of the inside pressure to 1 atm = 9.65 ml

Gas volume after evolution of O_2

= (38.43 + 9.65) - (1.55 + 1.50 + 2.80)

= 48.08 - 5.85

= 42.23 at $22.0^{o}C$

= 42.51 at $24.1^{o}C$

Volume of O_2 evolved

= 42. 51 - 39.18

= 3.33 ml at $24.1^{o}C$

= 3.03 ml at STP

= 3.03/0.0153

= 198.19 ml (STP)/gm product

Weight percent of Li_2O_2 in the product

$$= \frac{45.88 \quad 198.19}{22.4 \quad 10^3 \quad 0.5} \quad 100$$

= 81.39%

(3) Sample calculation for the determination of the peroxide in the product obtained from experiments with $Ca(OH)_2$

Discharge pressure = 0.30 torr

Flowrate of O_2 = 0.57 ml(STP)/min

Discharge power = 70 watts

Reaction time = 4 hrs

Product taken for analysis

= 8.80 mg

Gas buret reading at the ambient temperature (21.2°C) after attaching the reactor and adjustment of the inside pressure to 1 atm = 1.20 ml

Volume of the inside of the apparatus up to the zero mark of the buret = 38.43 ml

Total gas volume at 1 atm after attaching the reactor = 38.43 + 1.20

= 39.63 ml at 21.2°C

Volume of diethyl phthalate added

= 1.60 ml

Volume of acetic acid-dithyl phthalate mixture added = 1.45 ml

Volume of $FeCl_3$ solution added

= 3.00 ml

Gas buret reading at the ambient temperature (20.9°C) after evolution of O_2 and adjustment of the inside pressure to 1 atm.= 8.55 ml

Gas volume after evolution of O_2

$$= (38.43 + 8.55) - (1.60 + 1.45 + 3.00)$$

$$= 46.98 - 6.05$$

$$= 40.93 \text{ ml at } 20.9^{\circ}C$$

$$40.95 \text{ at } 21.2^{\circ}C$$

Volume of O_2 evolved

$$= 40.95 - 39.63$$

$$= 1.32 \text{ ml at } 21.2^{\circ}C$$

$$= 1.22 \text{ ml at STP}$$

$$= 1.22/0.0088$$

$$\approx 138.77 \text{ ml(STP)/gm}$$

Weight percent of CaO_2

$$= \frac{72.08 \quad 138.77}{22.4 \quad 10^3 \quad 0.5} \quad 100$$

$$= 87.97\%$$

NOMENCLATURE

A(s)	An arbitrary element in its solid form
b	Intensity parameter in the expression for B(r), kcal
B.M.	Bulk modulus, lbs/in^2
$B_2(g)$	A diatomic element in its gaseous form
B(r)	Potential function for repulsive interaction in the lattice, kcal
C	van der Waals interaction constant, (kcal).(cm)^6
C_p	Heat capacity, cal/(^{o}C)(mole)
ΔC_p	Difference of heat capacities of products and reactants, cal/(^{o}C)(mole)
$C_{p_{A(s)}}$	Heat capacity of A in its solid form, cal/(^{o}C)(mole)
$C_{p_{B_2(g)}}$	Heat capacity of gaseous B_2 cal/(^{o}C)(mole)
$C_{p_{AB_{2x}(s)}}$	Heat capacity of AB_{2x} in its solid form, cal/(^{o}C)(mole)
$C_{p_{Ca(g)}}$	Heat capacity of calcium vapor, cal/(^{o}C)(mole)
$C_{p_{Na(g)}}$	Heat capacity of sodium vapor, cal/(^{o}C)(mole)

$C_{p_{NaO_2(s)}}$	Heat capacity of sodium superoxide, cal/(^{o}C)(mole)
$C_{p_{O_2(g)}}$	Heat capacity of gaseous oxygen, cal/(^{o}C)(mole)
EA	Electron affinity, kcal
e	Charge of an electron, 1.6×10^{-19} coulomb
$\Delta F^{o}_{f,\ T}$	Standard free energy of formation at temperature T, kcal/mole
$\Delta F^{o}_{f,\ 298}$	Standard free energy of formation at 298^{o}K, kcal/mole
F_{O_2}	Flowrate of oxygen ml(STP)/min
$\Delta H^{o}_{f,\ T}$	Standard heat of formation at temperature T, kcal/mole
$\Delta H^{o}_{f,\ 298}$	Standard heat of formation at 298^{o}K, kcal/mole
ΔH^{o}_{T}	Standard heat of reaction at temperature T
ΔH_{sub}	Latent heat of sublimation, kcal/mole
IP	Ionization potential, kcal/mole
M	Madelung constant
m	Mass of sample taken for analysis, gram
M_s	Molecular weight of superoxide
M_p	Molecular weight of peroxide
N	Avogadro's number
p	Pressure, lbs/in^2
r	Interionic distance, $\mathring{A}$

r_a	Radius of anion, $\mathring{A}$
r_c	Radius of cation $\mathring{A}$
r_o	Equilibrium interionic distance, $\mathring{A}$
$S^o_{Ca(O_2)_2}$	Standard entropy of calcium superoxide
$\Delta S^o_{f,\ T}$	Standard entropy of formation at temperature T
$\Delta S^o_{f,\ 298}$	Standard entropy of formation at 298^oK
T	Temperature, ^oK
U	Lattice energy, kcal/mole
V	Volume of solid cm^3/mole
V_1	Volume of oxygen at STP released during the first step of wet chemical analysis of superoxide, ml
V_2	Volume of oxygen at STP released during the second step of wet chemical analysis of superoxide, ml
V_o	Equilibrium volume of solid, cm^3/mole
x_1	Number of moles of oxygen available due to decomposition of superoxide to peroxide
x_2	Number of moles of oxygen available due to decomposition of peroxide to monoxide or hydroxide

Greek Symbols

ρ	Range parameter in the repulsive potential B(r), $\mathring{A}$
$\phi(r)$	Potential function for the lattice energy
ϕ_o	Zero-point energy of the lattice, kcal

BIBLIOGRAPHY

1. Vol'nov, I. I., "Peroxide, Superoxides, and Ozonides of Alkali and Alkaline Earth Metals," Ed. Petrocelli, A. W., Plenum Press, New York, 1966.

2. Presti, J., Wellman, H. and Petrocelli, A. W., "Superoxide Life Support System for Submersibles," Undersea Technology,

3. Dieterly, D. K., et. al., "Potassium and Sodium Oxides for Oxygen Control in Manned Space Vehicles," NASA, Document No. N62-11085, 1962.

4. Snow, R. H., "Thermodynamic Evaluation of The Possibility of Lithium Superoxide Production," IIT Research Institute, Report No. IITRI- C6057-4, 1965.

5. Vol'nov, I. I., et. al., "Nature of The Reaction between Li_2O_2 and O_3," Izv. Akad. Nauk, Ser. Khim. 7, 1411 (1967).

6. Andrews, L., "Matrix Infrared Spectrum and Bonding in the Lithium Superoxide Molecule, LiO_2," J. Am. Chem. Soc. 90, 26 (1968).

7. Andrews, L. and Pimentel, G. C., "Infrared Spectrum, Structure, and Bonding of Lithium Nitroxide, LiON," J. Chem. Phys., 44, 6 (1966).

8. Weaver, R. D., Rewick, R. T. and Haynes, D. L. "Electrochemical Synthesis of Calcium Superoxide," Stanford Research Institute, Contract No. NAS2-7975.

9. Petrocelli, A. W. and Chiarenzelli, R., General Dynamics, Electric Boat Div., Report No. U-413-62-219, Dec. 31, 1962.

10. Wydeven, T., Personal Communication, Ames Research Center, Biotechnology Division, NASA, Moffett Field, CA.

11. Brosset, C. and Vannerberg, N. G., "Formation of Calcium Superoxide", Nature, 177, Feb. 4, 1956.

12. Vol'nov, I. I. and et. al., "Formation of Alkali Metal and Alkaline Earth Metal Peroxides and Superoxides during the Reaction of Hydroxides with Atomic Oxygen," Zh. Neorg. Khim. 12, 8 (1967)

13. Hollahan, J. and Wydeven, T., "Plasma Chemical Synthesis of Higher Oxides of Cesium and Rubidium," J. Inorg. Nucl. Chem. 35, 1079 (1973).

14. Latimer, W. M., "Methods of Estimating the Entropies of Solid Compounds," J. Am. Chem. Soc. 73, 1480 (1951).

15. D'Orazio, L. A. and Wood, R. H., "Thermodynamics of the Higher Oxides. I. The Heats of Formation and Lattice Energies of the Superoxides of Potassium, Rubidium, and Cesium," J. of Phys. Chem. 69, 8 (1965).

16. "International Critical Tables," McGraw Hill,

17. "Janaf Thermochemical Data," Dow Chemical Co., Midland, Michigan.

18. Evans, W. H. and et. al., "Thermodynamic Properties of the Alkali Metals," J. Res. National Bur. of Standards 55, 2 (1955).

19. Margrave, J. L., Chem. Eng. News 31, 39, 4012 (1953).

20. Born, M. and Mayer, J. E., Z. Physik 75, 1 (1932)

21. Ladd, M. F. C. and Lee, W. H., "The Calculation of Lattice Energies," J. Inorg. Nuel. Chem. 11, 264 (1959).

22. Cotton, F. A. and Wilkinson, G. "Advanced Inorganic Chemistry," 3rd Ed., Interscience Publishers, New York, 1972.

23. Pauling, L., "The Nature of the Chemical Bond," 3rd Ed., Cornell University Press, 1960.

24. Goldschmidt, V. M., "Geochemische Verteilungsgesetze de Elemente," Skrifter Norske Videnskaps-Akad. Oslo, I. Mat.-Naturv. Kl., 1926.

25. Carter, G. F. and Templeton, D. H., "Polymorphism of Sodium Superoxide," J. Am. Chem. Soc. 72, 2251 (1950).

26. Kittel, C., "Introduction to Solid State Physics," 4th Ed., John Willey and Sons, Inc., New York, 1973.

27. Bollnow, O. F., Z. Physik 33, 741 (1925).

28. Johnson, Q. C. and Templeton, D. H., "Madelung Constants for Several Structures," J. Chem. Phys. 34, 6 (1961).

29. Kubaschewski, O., Evans, E. and Alcock, C. B., "Metallurgical Thermochemistry," 4th Ed., Pergamon Press, New York, 1967.

30. Todd, S. S., "Heat Capacities at Low Temperatures and Entropies at 298.16°K of Sodium Superoxide, Potassium Superoxide and Sodium Peroxide," J. Am. Chem. Soc. 75, 1229 (1953).

31. Coughlin, J. P., "Contribution to the Data on Theoretical Metallurgy," US Bur. of Mines, Bulletin 542, 1954.

32. Seyb, E. and Kleinberg, J., "Determination of Superoxide Oxygen," Analytical Chem. 23, 1 (1951).

33. George, P. "Some Experiments on the Reactions of Potassium Superoxide in Aqueous Solutions," Discussions Faraday Soc. 2, 196 (1947).

34. Bell, A. T., "Fundamentals of Plasma Chemistry" in "Techniques and Applications of Plasma Chemistry," Ed. Hollhan, J. R. and Bell, A. T., John Wiley and Sons, Inc., 1974.

35. McTaggart, F. K., "Plasma Chemistry in Electrical Discharges," Elsevier Publishing Co., New York, 1967.

36. Valentine, D., "Annual Survey of Photochemistry," Interscience, 1970.

37. Kroger, C., Z. Anorg. Allgem. Chem. 253, 92 (1945).

38. Lux. H., Z. Anorg. Allgem. Chem., 298, 285 (1959).

39. Kazarnovskii, I. A., Zh. Fiz. Khim., 14, 333 (1940).

40. Brewer, A. K. and Westhaver, J. W., "Chemical Action in the Glow Discharge II. Further Investigation on the Synthesis of Ammonia," J. Phys. Chem. 34, 153 (1930).

41. Bell, A. T. and Kwong, K., "Dissociation of Oxygen in a Radiofrequency Electrical Discharge," AIChE Journal 18, 5 (1972).

42. Brown, L. C. and Bell, A. T., "Kinetics of the Oxidation of Carbon Monoxide and the Decomposition of Carbon Dioxide in a Radiofrequency Electric Discharge. I. Experimental Results," I & EC Fundamentals 13, 203 (1974).

43. Rode, T. V., "Thesis Reports of Third Conference on Physico-Chemical Analysis," Moscow, Izd. Akad. Nauk, P. 110, USSR (1955).

44. Marriott, J. A., Capotosto, A. and Petrocelli, A. W., "The Effect of Catalysts on the Thermal Decomposition of Sodium Superoxide," Anal. Chem. Acta. 41, 121 (1968).

45. "Handbook of Chemistry and Physics," 50th Ed., CRC.

46. "Properties of Potassium Superoxide," Brochure from Mine Safety Appliance Co., Evans city, Pa.

47. Blumenthal, M., Roczniki Chem. 12, 127 (1932).

48. de Forcrand, R., Compt. Rend. 158, 991 (1914).

49. Woolley, H. W., J. Res. National Bur. of Standards. 40, 163 (1948).

50. Gilles, P. W. and Margrave, J. L., "The Heats of Formation of Na_2O, NaO_2 and KO_2," J. Phys. Chem. 60, 1333 (1956).